Caspase-1 protein induces apoptosis-associated speck-like protein containing a caspase recruitment domain (ASC)-mediated necrosis independently of its catalytic activity

doi: 10.1074/jbc.M111.286823

Caspase-1 protein induces apoptosis-associated speck-like protein containing a caspase-recruitment domain (ASC)-mediated necrosis independently of its catalytic activity*

Kou Motani[‡], Hiroko Kushiyama[‡], Ryu Imamura[‡], Takeshi Kinoshita[‡], Takumi Nishiuchi[§], and Takashi Suda[‡]

From the [‡]Division of Immunology and Molecular Biology, Cancer Research Institute, Kanazawa University, Kakumamachi, Kanazawa, Ishikawa 920-1192, Japan and the [§]Division of Functional Genomics, Advanced Science Research Center, Kanazawa University, 13-1 Takaramachi, Kanazawa, Ishikawa 920-0934, Japan

Running title: Caspases determine the mode of ASC-mediated cell death

Address correspondence to: Takashi Suda, Division of Immunology and Molecular Biology, Cancer Research Institute, Kanazawa University, Kakumamachi, Kanazawa, Ishikawa 920-1192, Japan, Tel, 81-76-264-6720; FAX, 81-76-234-4525; E-mail: sudat@kenroku.kanazawa-u.ac.jp

Keywords: Necrosis, Apoptosis, Caspase, NLR, Tumor cell biology, Macrophages

Background: ASC mediates apoptosis and necrosis of tumor cells and necrosis of microbe-infected macrophages.
Result: ASC mediates necrosis only when cells express caspase-1; however, inhibition of caspase-1 proteolytic activity did not suppress the necrosis.
Conclusion: Caspase-1 but not is proteolytic activity is essential for ASC-mediated necrosis.
Significance: This paper explains why ASC induces apoptosis or necrosis depending on the cell type.

SUMMARY

The adaptor protein, apoptosis-associated speck-like protein containing a caspase-recruitment domain (ASC) connects pathogen/danger sensors such as NLRP3 and NLRC4 with caspases, and is involved in inflammation and cell death. We have found that ASC activation induced caspase-8-dependent apoptosis or CA-074Me (cathepsin B inhibitor)-inhibitable necrosis depending on the cell type. Unlike necroptosis, another necrotic cell death, ASC-mediated necrosis was neither RIP3-dependent nor necrostatin-1- inhibitable. Although Ac-YVAD-CMK (caspase-1 inhibitor) did not inhibit ASC-mediated necrosis, comprehensive gene-expression analyses indicated that caspase-1 expression coincided with the necrosis-type. Furthermore, caspase-1 knockdown converted necrosis-type cells to apoptosis-type, while exogenous expression of either wild-type or catalytically inactive caspase-1 did the opposite. Knockdown of caspase-1, but not Ac-YVAD-CMK, suppressed the monocyte necrosis induced by *Staphylococcus* and *Pseudomonas* infection. Thus, the catalytic activity of caspase-1 is dispensable for necrosis induction. Intriguingly, a short period of caspase-1 knockdown inhibited IL-1β production but not necrosis, although longer knockdown suppressed both responses. Possible explanations of this phenomenon are discussed.

ASC is an adaptor protein that connects several pattern recognition receptors (e.g., NLRP3, NLRC4) with caspase-1 (1,2). These pattern recognition receptors directly or indirectly recognize microbial molecular patterns (e.g. microbial RNA, flagellin) and/or danger signals from injured cells (e.g. ATP, uric acid), and then, together with ASC, they serve as platforms for the proteolytic maturation of caspase-1, which in turn catalyzes the proteolytic maturation of proinflammatory cytokines such as IL-1β and IL-18. Accordingly, ASC-deficient macrophages are severely defective in secreting these cytokines in response to microbial infection (3-5). Gain-of-function NLRP3 mutations cause auto-inflammatory syndromes, now collectively called cryopyrin-associated periodic syndromes (CAPS) (6). Importantly, IL-1 receptor antagonist has been shown to be effective in treating these syndromes. Thus, much attention has been paid to the role of ASC in caspase-1-mediated IL-1β maturation.

ASC also plays an important role in the monocyte and macrophage cell death induced by microbial infection. For instance, infection by an intracellular bacterium such as *Salmonella typhimurium*, *Pseudomonas (P.) aeruginosa*, or *Listeria monocytogenes* induces caspase-1-mediated cell death called “pyroptosis” (7-9). It has been described that pyroptosis has

characteristics of both necrosis (e.g. cell swelling and plasma membrane rupture) and apoptosis (nuclear shrinkage) (10). As expected from the fact that ASC plays an important role in caspase-1 activation, recent studies have demonstrated that ASC also plays an important role in pyroptosis (11,12). More recently, it was demonstrated that the expression of CAPS-associated NLRP3 mutants or the activation of endogenous NLRP3 by *Shigella flexneri* infection induces necrotic cell death in the THP-1 human monocytic cell line and/or mouse macrophages (13,14). This necrotic cell death is also mediated by ASC; however, it is inhibited by a cathepsin B inhibitor, CA-074Me but not by a caspase-1 inhibitor. Thus, this type of necrotic cell death has been considered to be distinct from pyroptosis, and it was named "pyronecrosis" (14).

Another line of studies demonstrated that ASC has the potential to induce apoptosis. ASC was originally identified as a protein that forms large aggregates in apoptotic human leukemia cells treated with chemotherapeutic agents (15), and as the product of a gene that is silenced in human cancer tissues by DNA methylation (16). In addition, it was demonstrated that ASC expression is induced by the p53 tumor suppressor, and is involved in etoposide-induced apoptosis (17). Thus, ASC-mediated apoptosis seems to be important for tumor suppression and for cancer cell chemosensitivity. Furthermore, we recently demonstrated that transplanted human tumors in nude mice were completely eradicated by ASC activation in the tumor cells (18). Thus, ASC is a promising molecular target for cancer therapy. We previously showed that oligomerization of ASC using an NLRC4-mimicry system induced caspase-8-mediated apoptosis in five human cancer cell lines, including the NUGC-4 gastric cancer cell line (19). More recently, we found that ASC activation using the NLRC4-mimicry system or a CAPS-associated mutant of NLRP3 induced necrotic cell death in the COLO205 human colon adenocarcinoma cell line (18).

In this study, we investigated the mode of cell death induced by NLRC4-mimicry in six other ASC-expressing tumor cell lines, and found that they were separated into apoptosis- and necrosis-type. We next sought to identify the molecular determinant of the mode of ASC-mediated cell death. We found that ASC activation induced necrosis in cells expressing caspase-1, but it induced caspase-8-dependent apoptosis in cells lacking caspase-1. Intriguingly, caspase-1, but not its catalytic activity, was essential for the ASC-mediated necrosis. The same was true for the ASC-dependent necrosis of the NOMO-1 human monocytic cell line induced by bacterial infection.

EXPERIMENTAL PROCEDURES

Reagents- An anti-human ASC mAb was prepared as described previously (20). Anti-caspase-1 polyclonal antibody (Cell Signaling, Beverly, MA), anti-cleaved caspase-1 mAb (clone D57A2, Cell Signaling), anti-β-actin mAb (clone AC-15, Sigma), anti-GAPDH mAb (clone MAB374, Millipore, Billerica, MA), MDP (Sigma, Saint Louis, MO), Z-IETD-FMK (R&D Systems, Minneapolis, MN), Ac-YVAD-CMK (Bachem, Torrance, CA), Z-DEVD-FMK, and CA-074Me (Merck Japan, Tokyo, Japan) were purchased.

Plasmids- The expression plasmids for Flag-C12N2, caspase-1, the caspase-1-C285S mutant, and pro-IL-1β were described previously (19,21-23). Lentiviral vectors expressing NLRP3 and NLRP3-Y570C were described previously (18). To generate lentiviral vectors expressing GFP, Flag-C12N2, caspase-1, and the caspase-1-C285S mutant, these cDNAs were inserted into pLenti6/V5-DEST (Invitrogen, Carlsbad, CA). To generate a plasmid expressing the GFP-Caspase-1 fusion protein (pEGFP-Casp1), the caspase-1 cDNA was cloned into a pEGFP-C1 vector (BD Clontech, Mountain View, CA). To generate lentiviral vectors expressing control and caspsae-1-targeting shRNA, oligo DNAs, including the corresponding sequences (CTAAGGTTAAGTCGCCCTCGCTCTAGCG AGGGCGACTTAACCTTAG, and ACACGTCTTGCTCTCATTATCTCGAGATA ATGAGAGCAAGACGTGT, respectively) were cloned into the pLKO.1 TRC vector (Addgene, Cambridge, MA).

Human cell lines- The NUC12N2 and CLC12N2 cell lines were described previously (18,19). The NUGC-4, COLO205, KLM-1 and MIAPaca2 cell lines were obtained from the Cell Resource Center for Biomedical Research, Tohoku University (Sendai, Miyagi, Japan). The C32TG, G-361, HMV-II, SK-MEL-28, and KU812 cell lines were obtained from the RIKEN BioResource Center (Ibaraki, Tsukuba,

Japan). The NOMO-1 cell line was obtained from the Health Science Research Resources Bank (Osaka, Japan). The THP-1 cell line was obtained from the American Type Culture Collection (Manassas, VA). To generate NOMO1-shCont and NOMO1-shCasp1 stable cell lines, NOMO-1 cells were transduced with a pLKO.1 lentiviral vector expressing control shRNA or caspase-1-targeting shRNA. The transduced cells were selected under puromycin treatment. The NU-GFP-Casp1 cell line was generated as follows: NUC12N2 cells were transfected with pEGFP-Casp1 using the Neon Transfection System (Invitrogen), and GFP-expressing cells were sorted by flow cytometry. To generate the NU-Casp1WT and NU-Casp1C285S cell lines, NUC12N2 cells were transduced with pLenti6/V5-DEST expressing the wild-type or C285S mutant of caspase-1. To generate the SKC12N2 cell line, SK-Mel-28 cells were transduced with pLenti6/V5-DEST expressing Flag-C12N2. The transduced cells were selected by blasticidin.

Apoptosis and necrosis assay- The mode of cell death (apoptosis or necrosis) was determined primarily by the morphology of the dying cells. The proportions of apoptotic and necrotic cells were determined by flow cytometry after staining with propidium iodide (PI) and Cy5-annexin V as described previously (18). PI(+)Cy5(-) cells and PI(-)Cy5(+) cells were considered necrotic and early apoptotic cells, respectively. PI(+)Cy5(+) cells were considered necrotic when increased PI staining preceded or occurred simultaneously with increased Cy5-Annexin V staining, whereas increased Cy5-Annexin V staining that preceded PI staining was considered to be an indication of the secondary necrosis of apoptotic cells. Otherwise, the proportions of apoptotic and necrotic cells were determined in situ after Hoechst33342 and PI staining, as described previously (18). A cell with a pyknotic nucleus without PI staining was considered apoptotic, while a PI(+) cell without profound nuclear condensation was considered necrotic. In some experiments, the proportion of necrosis was assessed by the release of cytoplasmic LDH into culture supernatants using the Cytotox 96 kit (Promega), according to the manufacturer's protocol. In some experiments, cell death was assessed by WST1 assay, as described previously (24).

Microarray analysis- Microarray analyses were performed using the Whole Human Genome Microarray Kit (G4100F, Agilent, Santa Clara, CA), according to the manufacturer's protocol. Total RNA was purified from CLC12N2 subclones (CLC12N2-Nec, CLC12N2-Apo) or from COLO205 and NUGC-4 cells using the RNeasy plus kit (Qiagen, Hilden, Germany). Cy3- and Cy5-labeled cRNAs were prepared using the Agilent Quick Amp Labeling Kit, Two-color (Agilent). Hybridization and analysis were performed as descried previously (25).

RT-PCR and real-time RCR- Total RNA was purified using TRIZOL reagent (Invitrogen), and cDNA was synthesized using the PrimeScript RT reagent Kit (Takara Bio, Shiga, Japan). The following primers were used for PCR: *ACTB*, 5'-TCCCTGGAGAAGAGCTACGA-3' and 5'-AAAGCCATGCCAATCTCATC-3'; *RIPK3*, 5'-TTTGGCCTGTCCACATTTCAG-3' and 5'-GGTTGGCAACTCAACTTCTCT-3'; *NLRP3*, 5'-TCTCATGGATTGGTGAACAGC-3' and 5'-GGTCCCCCAGAGAATTGTCA-3'; ASC (*PYCARD*), 5'-CTGGAGCCATGGGGCGCGCG-3' and 5'-CGGAGTGTTGCTGGGAAGGAG-3'; *NLRC4*, 5'-CAGCAAGTTGAATAAGCAAG-3' and 5'-ATCCTGTCGATCAGTTCATG-3'. Real-time PCR was performed using the THUNDERBIRD SYBR qPCR Mix (Toyobo, Osaka, Japan). The following primer sequences obtained from PrimerBank (http://pga.mgh.harvard.edu/primerbank/) were used for real-time PCR: *CASP1*, 5'-TCCAATAATGGACAAGTCAAGCC-3' and 5'-GCTGTACCCCAGATTTTGTAGCA-3'; *ACTB*, 5'-CATGTACGTTGCTATCCAGGC-3' and 5'-CTCCTTAATGTCACGCACGAT-3'.

Transfection of genes and siRNAs- Viral transduction was performed as described previously (18). CLC12N2 or NOMO-1 cells were transfected with siRNA (20 nM) using the Neon Transfection System. The ASC-targeting (HSS147064), NLRP3-targeting (HSS132811), and NLRC4-targeting (HSS126850) siRNAs were purchased from Invitrogen. The caspase-1-targeting siRNA (L-004401-00) was purchased from Dharmacon (Chicago, IL).

Measurement of IL-1β- The amount of human IL-1β in culture supernatants was determined using the OptEIA ELISA Kit (BD Pharmingen, San Diego, CA), according to the manufacturer's protocol.

Bacterial infection- Staphylococcus (S.) aureus (strain Smith, kindly provided by Dr. Nakanishi, Kanazawa University, Kanazawa, Ishikawa, Japan) and *P. aeruginosa* (JCM14847, Riken Bioresource Center, Wako, Saitama, Japan) in the log phase were used for infection. NOMO-1 and THP-1 cells were infected with these bacteria in antibiotic-free medium in 96-well plates. The plates were briefly centrifuged to improve the interaction between cells and bacteria. One hour after the infection, gentamycin (50 μg/ml) was added to kill the extracellular bacteria.

RESULTS

ASC activation induces apoptosis or necrosis in tumor cells derived from various tissues. To investigate ASC's functions, we previously established an experimental system in which a chimeric protein (C12N2) consisting of the caspase-recruitment domain from NLRC4, and the nucleotide-binding oligomerization domain and leucine-rich repeats from NOD2 (also called NLRC2), a sensor for muramyl dipeptide (MDP), was expressed in cells (20). In this system, the simple addition of MDP to the culture medium induces ASC-dependent responses in the cells. Hereafter, this system is termed NLRC4-mimicry. Using this system, we previously showed that ASC activation induces apoptosis in the NUGC-4 human stomach cancer cell line, but induced necrosis in the COLO205 human colon adenocarcinoma cell line (18). In the present study, we further investigated whether ASC activation induces apoptosis or necrosis in other ten tumor cell lines, including leukemia cell lines, melanomas, and pancreatic cancers. Among them, six expressed substantial amounts of ASC (Fig. 1*A*). These ten lines were transfected with C12N2 and treated with MDP. Among the six ASC-expressing lines, four (two monocytic leukemia cell lines, one melanoma, and one pancreatic cancer) exhibited necrosis, while two (melanomas) showed apoptosis (Fig. 1*B-E*, and see supplemental Fig. S1). MDP treatment without C12N2 transfection induced neither necrosis nor apoptosis in these cell lines (data not shown). Consistent with our previous findings (18,19), the NLRC4-mimicry-induced cell death of both apoptosis-type and necrosis-type cells was inhibited by ASC knockdown using siRNA (data not shown). The remaining cell lines, which expressed little or no ASC, were resistant to this procedure, confirming that the cell death induced by this procedure is ASC-dependent. These results indicate that ASC activation induces apoptosis or necrosis in ASC-expressing tumor cells of various tissue origins.

Effect of protease inhibitors on ASC-mediated cell death. We previously demonstrated that the ASC-mediated apoptosis of NUGC-4 cells was inhibited by a caspase-8 inhibitor, Z-IETD-FMK, while the ASC-mediated necrosis in COLO205 cells was inhibited by a cathepsin B inhibitor, CA-074Me (18). In addition, ASC has been implicated in pyroptosis that is inhibited by a caspase-1 inhibitor. Therefore, to further classify the type of cell death, we investigated the effect of these protease inhibitors. Consistent with our previous results, ASC-mediated cell death of all the apoptosis-type was inhibited by Z-IETD-FMK but not by CA-074Me (Fig. 2*A*). In contrast, the ASC-mediated cell death of necrosis-type cells was inhibited by CA-074Me, whereas neither Ac-YVAD-CMK nor Z-IETD-FMK inhibited it (Fig. 2*B*). These characteristics of ASC-mediated necrosis are shared with pyronecrosis.

The RIP1-RIP3 axis is not involved in the ASC-mediated necrosis. Death receptors that normally induce caspase-8-mediated apoptosis can elicit necrotic cell death (necroptosis), especially when caspases are inhibited. Necroptosis requires the expression of RIP1 and RIP3 (26-29), and is inhibited by a RIP1 inhibitor, necrostatin-1 (30). To investigate RIP3's involvement in ASC-mediated necrosis, we examined the RIP3 expression in tumor cell lines. RIP3 expression coincides with neither necrosis- nor apoptosis-type cells (Fig. 3*A*). In addition, necrostatin-1 did not inhibit the NLRC4-mimicry-induced necrosis in THP-1 cells, whereas it inhibited the necroptosis induced by TNF-α plus Z-VAD-FMK (pan-caspase inhibitor) in the same cell line (Fig. 3*B*). These results indicate that ASC-mediated necrosis is distinct from necroptosis.

Caspase-1 expression correlates with the necrotic phenotype. The stable transfectants of COLO205 cells expressing C12N2 (CLC12N2) exhibit necrosis in response to MDP stimulation (18). By limiting dilution, we obtained one subclone of CLC12N2 cells that exhibited necrosis (CLC12N2-Nec) just like the parental CLC12N2 cells and another subclone that exhibited apoptosis (CLC12N2-Apo) upon ASC activation (Fig. 4*A* and see supplemental Movie S1 and Movie S2). Consistent with our previous conclusion that ASC-mediated apoptosis is caspase-8- dependent (19), Z-IETD-FMK inhibited the cell death of CLC12N2-Apo but not CLC12N2-Nec cells (Fig. 4*B*).

To identify what determines the mode of ASC-mediated cell death, we compared the gene expression profiles between CLC12N2-Nec and CLC12N2-Apo cells and between the original COLO205 (necrosis-type) and NUGC-4 cells (apoptosis-type). We first selected those genes that expressed either more or less consistently in CLC12N2-Nec compared to CLC12-Apo cells and in COLO205 cells compared to NUGC-4 cells. Among them, the top 10 genes with the greatest difference in expression between the CLC12N2-Nec and CLC12-Apo cells are shown in Fig. 4*C*. Using real-time PCR, we examined the expression of these 20 genes in other tumor cell lines. To our surprise, *CASP1* was the only gene that completely coincided with the necrosis-type cell lines (Fig. 4*D* and see supplemental Fig. S2). Although CARD16 expression had a weak correlation with the necrosis-type, CARD16 knockdown did not inhibit the MDP-induced necrosis of CLC12N2-Nec cells (see supplemental Fig. S3), suggesting that CARD16 is not required for ASC-mediated necrosis. No gene completely coincided with the apoptotic phenotype (see supplemental Fig. S4). Western blot analyses confirmed that substantial amounts of caspase-1 protein were expressed in the necrosis-type but not apoptosis-type cell lines (Fig. 4*E*). We previously reported that NLRC4-mimicry induces apoptosis in four gastrointestinal cancer cell lines, including NUGC-4, and one lung cancer cell line (19). Consistent with the above results, all of these cell lines expressed no caspase-1 (see supplemental Fig. S5). Therefore, caspase-1 is a novel cellular factor determining the mode of cell death.

Caspase-1 is required for ASC-mediated necrosis. To investigate whether caspase-1 is required for ASC-mediated necrosis, caspase-1 expression in CLC12N2-Nec cells was down-regulated using siRNA. Although the one-time transfection of caspase-1-targeting siRNA but not control siRNA severely reduced the expression of caspase-1 protein, the NLRC4-mimicry-induced necrosis was only slightly suppressed by the caspase-1-targeting siRNA (Fig. 5*A*). However, after a 6- or 9-day culture with repetitive siRNA transfection, the necrosis was reduced and, interestingly, apoptosis gradually increased. These results suggest that a special caspase-1 with a long half-life is involved in ASC-mediated necrosis. To confirm the role of caspase-1 in ASC-mediated necrosis, we introduced a GFP-caspase-1 fusion gene into NUC12N2 cells (C12N2-expressing NUGC-4 cells), and thereby established NU-GFP-Casp1 cells. MDP stimulation induced apoptosis in NUC12N2 cells, but induced necrosis in NU-GFP-Casp1 cells (Fig. 5*B*). Thus, exogenous caspase-1 expression converted apoptosis-type cells to necrosis-type.

CAPS-associated NLRP3 mutants induce necrotic cell death in the human monocytic leukemia cell line THP-1 (13,14). Here we found that one such mutant, NLRP3-Y570C, but not the wild-type NLRP3, induced necrosis in another human monocytic cell line, NOMO-1. Consistent with the NLRC4-mimicry-induced necrosis of CLC12N2 cells, the NLRP3-Y570C -induced necrosis was suppressed by ASC-targeting siRNA (Fig. 5*C*) and stable expression of caspase-1-targeting shRNA (Fig. 5*D*), whose target sequence was completely different from that of the caspase-1-targeting siRNA used above. Furthermore, the NLRP3-Y570C-induced necrosis was converted to apoptosis by suppressing caspase-1 expression (Fig. 5*E*, *F*). Z-IETD-FMK inhibited the apoptosis observed in caspase-1-deficient cells, but not the necrosis observed in the caspase-1-sufficient cells (Fig. 5*F*), indicating that ASC activation induces caspase-8-dependent apoptosis in cells lacking caspase-1.

Caspase-1 catalytic activity is not required for ASC-mediated necrosis. Because Ac-YVAD-CMK did not inhibit the NLRC4-mimicry-induced cell death of necrosis-type cell lines (Fig. 2*B*), we next investigated whether the catalytic activity of

caspase-1 is involved in ASC-mediated necrosis. When SK-Mel-28 (SKC12N2) cells expressing C12N2 were treated with MDP, a fragment (p20) of mature caspase-1 was detected in the cell lysate and culture supernatant (Fig. 6*A*). Treatment with 40 μM Ac-YVAD-CMK completely inhibited the caspase-1 processing, but did not inhibit the ASC-mediated necrosis of SKC12N2 cells (Fig. 6*B*), supporting the notion that the caspase-1 catalytic activity is not required for ASC-mediated necrosis. To further confirm this notion, wild-type caspase-1, the catalytically inactive caspase-1-C285S mutant, or GFP was transduced into NUC12N2 cells using a lentiviral vector. The exogenous caspase-1 expression levels were comparable to those of endogenous caspase-1 in COLO205 and SK-Mel-28 cells (Fig. 6*C* and see supplemental Fig. S6*A*). Both the wild-type and C285S mutant of caspase-1 converted the mode of NLRC4-mimicry-induced cell death from apoptosis to necrosis, but GFP did not (Fig. 6*D* and see supplemental Fig. S6*B*). These cells were further transfected with an expression plasmid for proIL-1β, and then stimulated with MDP. Importantly, cells expressing the wild-type, but not the mutant caspase-1, secreted IL-1β (Fig. 6*E*), confirming that the C285S mutant was catalytically inactive. These results indicate that the catalytic activity of caspase-1 is not required for ASC-mediated necrosis.

Caspase-1, but not its catalytic activity, is essential for the ASC-mediated necrosis of S. aureus-infected monocytes. *S. aureus* α-haemolysin induces NLRP3- and ASC-dependent pyronecrosis in THP-1 cells (31). This necrotic cell death was reported to be caspase-1-independent, because it was not inhibited by Z-VAD-FMK. Therefore, we next investigated the role of caspase-1 and its catalytic activity in the *S. aureus*-induced death of NOMO-1 cells. Consistent with the previous report (31), the *S. aureus*-induced cell death exhibited a necrotic morphology (Fig. 7*A*), and this necrosis was inhibited by siRNAs for ASC and NLRP3 but not for NLRC4 (Fig. 7*B*). Similar to NLRC4-mimicry-induced necrosis, the *S. aureus*-induced necrosis was inhibited by CA-074Me, but not by Z-IETD-FMK (Fig. 7*C*). In addition, a caspase-3 inhibitor, Z-DEVD-FMK did not inhibit the *S. aureus*-induced necrosis, indicating that caspase-3, the executioner of apoptosis, was not involved in this cell death (Fig. 7*C*). Furthermore, Ac-YVAD-CMK that was sufficient to inhibit IL-1β production did not inhibit the *S. aureus*-induced necrosis (Fig. 7*D*). Similar results were obtained using THP-1 cells (see supplemental Fig. S7). Nonetheless, the *S. aureus*-induced necrosis was suppressed by caspase-1 knockdown (Fig. 7*E*). These results indicate that the *S. aureus*-induced necrosis requires caspase-1 but not its catalytic activity. Consistent with our observations in NLRC4-mimicry-induced necrosis, a short period of caspase-1 knockdown inhibited the *S. aureus*-induced IL-1β production but not necrosis, while longer knockdown suppressed both responses (Fig. 7*F*). However, *S. aureus*-induced necrosis was not inhibited even after 7 or 12-day exposure of NOMO-1 cells to Ac-YVAD-CMK (see supplemental Fig. S8), supporting further that the catalytic activity of caspase-1 is not required for the ASC-mediated necrosis.

Caspase-1, but not its catalytic activity, is required for the NLRC4-dependent, ASC-independent necrosis of P. aeruginosa-infected monocytes. It was reported that *P. aeruginosa* infection induces NLRC4- and caspase-1-dependent pyroptosis in macrophages (32). Consistent with the report, we observed that *P. aeruginosa* induced necrosis in NOMO-1 cells (Fig. 7*G*), and this necrosis was inhibited by NLRC4-targeting siRNA but not by ASC- or NLRP3-targeting siRNA (Fig. 7*H*), although the necrosis observed after *P. aeruginosa* infection at a low multiplicity of infection (moi) was strongly suppressed by both NLRC4- targeting and ASC-targeting siRNAs (data not shown). Consistent with the above *S. aureus* infection model, the *P. aeruginosa*-induced necrosis was suppressed in NOMO-1 cells carrying the caspase-1-targeting shRNA (Fig. 7*I*). However, Ac-YVAD-CMK that was sufficient to inhibit IL-1β production did not inhibit the *P. aeruginosa*-induced necrosis (Fig. 7*J*). Thus, the caspase-1 catalytic activity is also dispensable for NLRC4-mediated pyroptosis.

DISCUSSION

In this study, we discovered that activation of ASC induces necrosis when cells express caspase-1, otherwise the same induces apoptosis. Thus, caspase-1 is a novel molecular determinant of cell death modes. Intriguingly,

we found that ASC-mediated necrosis does require caspase-1 expression, but not its catalytic activity. This conclusion was confirmed by experiments using a caspase-1 inhibitor and a catalytically inactive caspase-1 mutant. This is the first report of a catalytic activity-independent function of caspase-1. A caveat is that our results do not exclude the possibility that there are caspase-1 catalytic activity-dependent mechanisms of pyroptosis in addition to the catalytic activity-independent one. This concern is analogous to the fact that caspase-dependent DNase, which causes DNA degradation during apoptosis and hence would cause cell death, is not essential for the cell death itself (33).

In contrast to our conclusion described above, it has been thought that pyroptosis of human monocytes requires caspase-1 catalytic activity. This conclusion has been drawn from experiments using high concentrations (50-200 μM) of Z-VAD-FMK or Ac-YVAD-CMK (11, 34). Such high concentrations of these inhibitors could non-specifically inhibit other proteases including cathepsin B (35). Thus, the requirement of caspase-1 catalytic activity in pyroptosis of human macrophages should be re-evaluated using a lower dose of Ac-YVAD-CMK. Recently, Broz et al demonstrated that autoproteolysis of caspase-1 is required for IL-1β processing but not for pyroptosis of mouse macrophages infected by *Salmonella* or *Legionella*, although the proteolytic activity of caspase-1 was required for both responses (36). In addition, they demonstrated that formation of a large focus of ASC was required for IL-1β production, whereas formation of NLRC4-caspase1 complexs was sufficient and ASC was not required for the cell death. Broz's and our results are similar in that both indicate that the use of caspase-1 in IL-1β processing and cell death is somewhat different. However, they were different from each other in the requirement of the proteolytic activity of caspase-1 for cell death. This difference may be species difference. Actually, our preliminary experiments using mouse peritoneal macrophages showed that low concentrations (2-10 μM) of Ac-YVAD-CMK significantly inhibited *Salmonella typhimurium*- and *P. aeruginosa*-induced cell death, albeit less efficiently than it inhibited IL-1β release under the same conditions (see supplemental Fig. S9). In Broz's experimental system, macrophages were killed in an ASC-independent manner. In contrast, we mainly investigated ASC-dependent necrosis in this study. However, the difference in ASC-dependency is unlikely to be a reason for the different requirement in terms of the caspase-1 proteolytic activity for necrosis, because ASC-independent necrosis of *P. aeruginosa*-infected NOMO-1 cells was not inhibited by Ac-YVAD-CMK (Fig. 7J).

On the other hand, pyronecrosis has been mainly characterized using THP-1 cells infected with *Shigella flexneri*, *Neisseria gonorrhoeae* or adenovirus, or treated with *S. aureus* α-haemolysin (14,31,37,38). Pyronecrosis has been concluded to be caspase-1-independent, mainly because these cases of cell death were not inhibited by Z-VAD-FMK or Ac-YVAD-CMK at relatively low concentrations sufficient to inhibit caspase-1-mediated IL-1β secretion. Whether macrophages from caspase-1-deficient mice are resistant to *Shigella*-induced cell death has been controversial (14,39). In other experimental systems of pyronecrosis, the requirement for caspase-1 expression has not been examined. Thus, the requirement for caspase-1 in the pyronecrosis observed in the above experimental systems needs to be re-examined.

Both pyroptosis and pyronecrosis are mediated by NLRs and ASC, and are accompanied by IL-1β production. Morphologically, both modes of cell death are characterized by rapid cell swelling followed by plasma-membrane rupture. Nuclear shrinkage has been observed for pyroptosis. However, it has not been clearly described whether pyronecrosis is also accompanied by nuclear shrinkage. Therefore, one cannot distinguish pyroptosis and pyronecrosis solely by the morphology of the dying cells. We observed nuclear shrinkage in some cells undergoing ASC-mediated necrosis. We found that all the instances of ASC-mediated necrosis examined in our study were inhibited by CA-074Me. This is a characteristic of pyronecrosis. However, it was recently reported that pyroptosis is also inhibited by CA-074Me (40). The sole factor that clearly discriminated the two modes of cell death was that caspase-1 was essential for pyroptosis, but not pyronecrosis. However, this distinction is now questionable as described above. Based on our results presented here, it is likely that pyroptosis and pyronecrosis are the same mode of cell death. The molecular mechanisms of pyroptosis and pyronecrosis

have not been well understood. Our finding that caspase-1 is capable of inducing necrosis independently of its catalytic activity may provide important insight into the molecular mechanism of these necrotic cell death modes.

ASC-mediated necrosis induced by NLRC4-mimicry in CLC12N2 cells and by the NLRP3-Y570C mutant in NOMO-1 cells was converted to apoptosis when caspase-1 expression was suppressed by RNA interference. However, the ASC-mediated necrosis induced by *S-aureus* infection in NOMO-1 cells was merely suppressed, not converted to apoptosis, by reduced caspase-1 expression. One possible explanation for these distinctive outcomes by different stimuli in the same cell line is that the host cells or microbes in *S. aureus*-infected NOMO-1 cells might produce something that inhibits caspase-8 activation. Further study is required to clarify this point.

Although CA-074Me, the well-known cathepsin B inhibitor abrogated ASC-mediated necrosis, there was no correlation between cathepsin B expression and the mode of ASC-mediated cell death (see supplemental Fig, S10*A*). It should be note that whether cathepsin B plays an essential role in this type of cell death is not clear, because we previously found that knockdown of cathepsin B expression using siRNA failed to inhibit the MDP-induced cell death of CLC12N2 cells (18). Consistently, knockdown of cathepsin B in NOMO1-C12N2 cells also failed to inhibit the MDP-induced cell death (see supplemental Fig. S10*B*). Thus, further experiments are required to determine the target of CA-074Me in the inhibition of ASC-mediated necrosis.

Here, we found that a short-term knockdown of caspase-1 abrogated IL-1β production but not ASC-mediated necrosis, whereas its long-term knockdown diminished both responses. Thus, the caspase-1 involved in necrosis might have a longer half-life compared to that involved in IL-1β secretion. Alternatively, the absence of caspase-1 might result in gradual decrease of the amount and/or activity of another molecule that was essential for the ASC-mediated necrosis. Further study aiming to explain this interesting phenomenon may provide a clue to the molecular mechanism of caspase-1-meidated necrosis.

References

1. Schroder, K., and Tschopp, J. (2010) *Cell.* **140**, 821-832
2. Franchi, L., Eigenbrod, T., Munoz-Planillo, R., and Nunez, G. (2009) *Nat. Immunol.* **10**, 241-247
3. Mariathasan, S., Newton, K., Monack, D. M., Vucic, D., French, D. M., Lee, W. P., Roose-Girma, M., Erickson, S., and Dixit, V. M. (2004) *Nature* **430**, 213-218
4. Özören, N., Masumoto, J., Franchi, L., Kanneganti, T.-D., Body-Malapel, M., Erturk, I., Jagirdar, R., Zhu, L., Inohara, N., Bertin, J., Coyle, A., Grant, E. P., and Nunez, G. (2006) *J. Immunol.* **176**, 4337-4342
5. Yamamoto, M., Yaginuma, K., Tsutsui, H., Sagara, J., Guan, X., Seki, E., Yasuda, K., Yamamoto, M., Akira, S., Nakanishi, K., Noda, T., and Taniguchi, S. (2004) *Genes Cells* **9**, 1055-1067
6. Hoffman, H. M., and Wanderer, A. A. (2010) *Curr. Allergy Asthma Rep.* **10**, 229-235
7. Brennan, M. A., and Cookson, B. T. (2000) *Mol. Microbiol.* **38**, 31-40
8. Franchi, L., Stoolman, J., Kanneganti, T.-D., Verma, A., Ramphal, R., and Nunez, G. (2007) *Eur. J. Immunol.* **37**, 3030-3039
9. Cervantes, J., Nagata, T., Uchijima, M., Shibata, K., and Koide, Y. (2008) *Cell. Microbiol.* **10**, 41-52
10. Bergsbaken, T., Fink, S. L., and Cookson, B. T. (2009) *Nat. Rev. Microbiol.* **7**, 99-109
11. Fernandes-Alnemri, T., Wu, J., Yu, J. W., Datta, P., Miller, B., Jankowski, W., Rosenberg, S., Zhang, J., and Alnemri, E. S. (2007) *Cell Death Differ.* **14**, 1590-1604
12. Sauer, J.-D., Witte, C. E., Zemansky, J., Hanson, B., Lauer, P., and Portnoy, D. A. (2010) *Cell Host Microbe* **7**, 412-419
13. Fujisawa, A., Kambe, N., Saito, M., Nishikomori, R., Tanizaki, H., Kanazawa, N., Adachi, S., Heike, T., Sagara, J., Suda, T., Nakahata, T., and Miyachi, Y. (2007) *Blood* **109**, 2903-2911
14. Willingham, S. B., Bergstralh, D. T., O'Connor, W., Morrison, A. C., Taxman, D. J., Duncan, J. A., Barnoy, S., Venkatesan, M. M., Flavell, R. A., Deshmukh, M., Hoffman, H. M., and Ting, J. P. -Y. (2007) *Cell Host Microbe* **2**, 147-159
15. Masumoto, J., Taniguchi, S., Ayukawa, K., Sarvotham, H., Kishino, T., Niikawa, N., Hidaka, E., Katsuyama, T., Higuchi, T., and Sagara, J. (1999) *J. Biol. Chem.* **274**, 33835-33838
16. Conway, K. E., McConnell, B. B., Bowring, C. E., Donald, C. D., Warren, S. T., and Vertino, P. M. (2000) *Cancer Res.* **60**, 6236-6242
17. Ohtsuka, T., Ryu, H., Minamishima, Y. A., Macip, S., Sagara, J., Nakayama, K. I., Aaronson, S. A., and Lee, S. W. (2004) *Nat. Cell Biol.* **6**, 121-128
18. Motani, K., Kawase, K., Imamura, R., Kinoshita, T., Kushiyama, H., and Suda, T. (2010) *Cancer Sci.* **101**, 1822-1827
19. Hasegawa, M., Kawase, K., Inohara, N., Imamura, R., Yeh, W.-C., Kinoshita, T., and Suda, T. (2007) *Oncogene* **26**, 1748-1756
20. Imamura, R., Wang, Y., Kinoshita, T., Suzuki, M., Noda, T., Sagara, J., Taniguchi, S', Okamoto, H., and Suda, T. (2010) *J. Immunol.* **184**, 5874-5884
21. Hasegawa, M., Imamura, R., Kinoshita, T., Matsumoto, N., Masumoto, J., Inohara, N., and Suda, T. (2005) *J. Biol. Chem.* **280**, 15122-15130
22. Wang, Y., Hasegawa, M., Imamura, R., Kinoshita, T., Kondo, C., Konaka, K., and Suda, T. (2004) *Int. Immunol.* **16**, 777-786
23. Kinoshita, T., Wang, Y., Hasegawa, M., Imamura, R., and Suda, T. (2005) *J. Biol. Chem.* **280**, 21720-21725
24. Fukui, M., Imamura, R., Umemura, M., Kawabe, T., and Suda, T. (2003) *J. Immunol.* **171**, 1868-1874
25. Hasegawa, M., Imamura, R., Motani, K., Nishiuchi, T., Matsumoto, N., Kinoshita, T., and Suda, T. (2009) *J. Immunol.* **182**, 7655-7662
26. Hitomi, J., Christofferson, D. E., Ng, A., Yao, J., Degterev, A., Xavier, R. J., and Yuan, J. (2008) *Cell* **135**, 1311-1323
27. He, S., Wang, L., Miao, L., Wang, T., Du, F., Zhao, L., and Wang, X. (2009) *Cell* **137**, 1100-1111
28. Cho, Y. S., Challa, S., Moquin, D., Genga, R., Ray, T. D., Guildford, M., and Chan, F. K.-M. (2009) *Cell* **137**, 1112-1123
29. Zhang, D.-W., Shao, J., Lin, J., Zhang, N., Lu, B.-J., Lin, S.-C., Dong, M.-Q., and Han, J. (2009) *Science* **325**, 332-336
30. Degterev, A., Hitomi, J., Germscheid, M., Ch'en, I. L., Korkina, O., Teng, X., Abbott, D., Cuny, G. D., Yuan, C., Wagner, G., Hedrick, S. M., Gerber, S. A., Lugovskoy, A., and Yuan, J. (2008) *Nat. Chem. Biol.* **4**, 313-321

31. Craven, R. R., Gao, X., Allen, I. C., Gris, D., Bubeck Wardenburg, J., McElvania-Tekippe, E., Ting, J. P., and Duncan, J. A. (2009) *PLoS One* **4**, e7446
32. Sutterwala, F. S., Mijares, L. A., Li, L., Ogura, Y., Kazmierczak, B. I., and Flavell, R. A. (2007) *J. Exp. Med.* **204**, 3235-3245
33. McIlroy, D., Sakahira, H., Talanian, R. V., and Nagata, S. (1999) *Oncogene* **18**, 4401-4408
34. Kelk, P., Johansson, A., Claesson, R., Hanstrom, L., and Kalfas, S. (2003) *Infect. Immun.* **71**, 4448-4455
35. Schotte, P., Declercq, W., Van Huffel, S., Vandenabeele, P., and Beyaert, R. (1999) *FEBS Lett.* **442**, 117-121
36. Broz, P., von Moltke, J., Jones, J. W., Vance, R. E., and Monack, D. M. (2010) *Cell Host Microbe* **8**, 471-483
37. Duncan, J. A., Gao, X., Huang, M. T.-H., O'Connor, B. P., Thomas, C. E., Willingham, S. B., Bergstralh, D. T., Jarvis, G. A., Sparling, P. F., and Ting, J. P.-Y. (2009) *J. Immunol.* **182**, 6460-6469
38. Barlan, A. U., Griffin, T. M., McGuire, K. A., and Wiethoff, C. M. (2011) *J. Virol.* **85**, 146-155
39. Hilbi, H., Moss, J. E., Hersh, D., Chen, Y., Arondel, J., Banerjee, S., Flavell, R. A., Yuan, J., Sansonetti, P. J., and Zychlinsky, A. (1998) *J. Biol. Chem.* **273**, 32895-32900
40. Averette, K. M., Pratt, M. R., Yang, Y., Bassilian, S., Whitelegge, J. P., Loo, J. A., Muir, T. W., and Bradley, K. A. (2009) *PLoS One* **4**, e7913

FOOTNOTES

* This work was supported in part by Grants-in-Aid for Scientific Research on Priority Areas (Cancer) from the Ministry of Education, Culture, Sports, Science and Technology, the Japanese Government.

The Abbreviations used are: ASC, apoptosis-associated speck-like protein containing a caspase-recruitment domain, CAPS, cryopyrin-associated periodic syndromes; MDP, muramyl dipeptide; moi, multiplicity of infection; *P, Pseudomonas*; *S, Staphylococcus*; PI, propidium iodide

FIGURE LEGENDS

FIGURE 1. ASC activation induces apoptosis or necrosis in various tumor cell lines. *A,* ASC and β-actin levels were examined by Western blotting. *B-E,* The indicated cell lines were transduced with a lentiviral vector expressing C12N2. The cells were then treated with or without MDP (100 ng/ml). *B,* Cell morphology was examined under a microscope. Representative necrotic and apoptotic cells are shown by arrows and arrowheads, respectively. Scale bars, 20 μm. *C,* Leukemia and melanoma cell lines were stained with propidium iodide (PI) and Cy5-annexin V, and the percentages of apoptotic and necrotic cells were determined by flow cytometry. The staining profiles are shown in supplemental Fig. S1. *D,* Pancreatic cancer cell lines were stained with Hoechst33342 and PI, and examined under a fluorescence microscope. Necrotic cells (arrows) had morphologically normal nuclei that were stained with PI. Scale bar in the top left panel, 20 μm. *E,* Apoptotic and necrotic cells were counted under a fluorescence microscope. At least 500 total cells were counted for each group. *Error bars* in *C* and *E* indicate S.D.

FIGURE 2. Effect of protease inhibitors on ASC-mediated cell death. *A,* NUGC-4, HMV-II, and G-361 cells expressing C12N2 were left untreated or were treated with 40 μM of Z-IETD-FMK or CA-074Me for 1 h, and were then cultured with or without MDP (100 ng/ml) for 12 h. The proportion of apoptotic cells was determined as described in Fig. 1*C*. *B,* COLO205, THP-1, NOMO-1, and SK-Mel-28 cells expressing C12N2 were pre-treated with the indicated inhibitors (20, 40 and 80 μM) for 1 h, and then cultured with or without MDP (100 ng/ml) for 8 h. Cell viability was assessed by WST-1 assay. Cell Death (%) = {(A_{450} of cell culture without MDP - A_{450} of cell culture with MDP) / A_{450} of cells cultured without MDP} x 100. *Error bars* in *A* and *B* indicate S.D.

FIGURE 3. The RIP1-RIP3 axis is not involved in ASC-mediated necrosis. *A,* The RIP3 (*RIPK3*) and β-actin (*ACTB*) mRNA levels in the indicated tumor cell lines were analyzed by RT-PCR. *B,* THP-1 cells (left) or C12N2-expressing THP-1 cells (right) were pre-treated with necrostatin-1 (10 μM) for 1 h. Then, the THP-1 cells were treated with recombinant mouse TNF-α (30 ng/ml) and Z-VAD-FMK (40 μM) for 48 h, while the C12N2-expressing THP-1 cells were treated with MDP (100 ng/ml) for 10 h. Cell viability was assessed by

WST-1 assay as described in Fig. 2*B*. *Error bars* indicate S.D.

FIGURE 4. Caspase-1 expression correlates with the necrotic phenotype. *A,* CLC12N2-Apo and CLC12N2-Nec cells were treated with MDP (100 ng/ml) for 12 h, then analyzed as described in Fig. 1*B*. *B*, CLC12N2-Apo and CLC12N2-Nec cells were pre-treated with Z-IETD-FMK (5, 10, 20, or 40 μM) for 1 h or left untreated, and then were treated with MDP (100 ng/ml) for 12 h. The percentages of apoptotic and necrotic cells were determined by flow cytometry. *C,* Gene expression profiles of CLC12N2-Nec and CLC12N2-Apo cells or COLO205 and NUGC-4 cells were compared by DNA-microarray analyses. The top 10 genes with greater expression in CLC212N2-Nec cells than in CLC12N2-Apo cells are listed in the upper panel, while those expressed more in CLC12N2-Apo cells than in CLC12N2-Nec cells are shown in the lower panel. Numbers shown are the fold difference in gene expression levels between the indicated cell lines. Original datasets of the microarray analyses are available at CIBEX (http://cibex.nig.ac.jp/index.jsp, accession no. CBX131). *D,* The caspase-1 mRNA levels relative to that of β-actin, as determined by quantitative RT-PCR, are shown for the indicated cell lines. *E,* Caspase-1 and β-actin protein levels in the indicated cells were examined by Western blotting. *Error bars* in *B* and *D* indicate S.D.

FIGURE 5. Caspase-1 with a long half-life is required for ASC-mediated necrosis. *A,* CLC12N2-Nec cells were transfected with control (*siCont, circles*) or caspase-1-targeting siRNA (*siCasp1, triangles*) 1–3 times at 3-day intervals. At 3, 6, or 9 days after the first transfection, the cells were treated with MDP (100 ng/ml) for 12 h, and the proportions of apoptotic (open symbols) and necrotic cells (closed symbols) were determined by flow cytometry as described in Fig. 1*B*. Caspase-1 (*Casp1*) and GAPDH expression levels at the indicated times before MDP stimulation were examined by Western blotting (lower panels). *B,* NUC12N2 and NU-GFP-Casp1 cells were treated with MDP (1000 ng/ml) or left untreated for 6 h, then stained with Hoechst33342 and PI, and examined under a fluorescence microscope. The upper and lower panels show Hoechst- and PI-stained images, respectively. Apoptotic cells had pyknotic nuclei that were brightly stained with Hoechst33342 but not with PI, while necrotic cells had morphologically normal nuclei that were stained with PI. Scale bar, 20 μm. GFP-caspase-1 (*GFP-Casp1*) and GAPDH expression levels in these cells before MDP stimulation were examined by Western blotting (lower panels). *C,* NOMO-1 cells treated with control or ASC-targeting siRNA (*siASC*) for 72 h were transduced with empty lentiviral vector (*Vector*), or with the vector expressing wild-type (wt) NLRP3 or its Y570C mutant (mt). Twelve hours after transduction, cytotoxicity was assessed by LDH release (upper panel). ASC and GAPDH expression levels were examined by Western blotting 48 h after the siRNA transfection (lower panels). *D* and *E*, NOMO1-shCont and NOMO1-shCasp1 cells were transduced with an empty lentiviral vector or one expressing the wild-type or Y570C mutant of NLRP3, and were cultured for 12 h. *D,* Cytotoxicity was assessed as described in (*C*). Caspase-1 and GAPDH levels were examined by Western blotting (lower panels). *E,* Cells were examined as described in (*B*). Scale bar, 20 μm. Arrowheads indicate apoptotic cells. *F,* NOMO1-shCont and NOMO1-shCasp1 cells were pre-treated with Z-IETD-FMK (40 μM) or DMSO (solvent control) for 1 h. Cells were then transduced with a lentiviral vector expressing the Y570C mutant of NLRP3, and were further cultured for 12 h. Apoptotic and necrotic cells were counted under a fluorescence microscope. *Error bars* in *A, C, D* and *F* indicate S.D.

FIGURE 6. Caspase-1 catalytic activity is not required for ASC-mediated necrosis. *A,* SK-Mel-28 cells stably expressing C12N2 (SKC12N2) were treated with MDP (1000 ng/ml) for the indicated period. The large subunit of mature caspase-1 (p20) in cell lysates and culture supernatants was detected by Western blotting. *B*, SKC12N2 cells were left untreated or were pre-treated with Ac-YVAD-CMK (40 μM), and then stimulated with MDP (1000 ng/ml) for 4 h. Cytotoxicity was assessed by an LDH release assay, and caspase-1 p20 in culture supernatants was detected by Western blotting. *C* and *D*, NUC12N2 cells were transduced with a lentiviral vector expressing GFP, wild-type caspase-1 or the C285S mutant of caspase-1. *C,* Caspase-1 and β-actin levels in the indicated cells were examined by Western blotting. *D,* NUC12N2 cells expressing GFP, wild-type caspase-1 (WT) or the C285S mutant of caspase-1 (CS) were cultured with MDP (1000 ng/ml) for 6 h, and then stained with Hoechst33342 and PI. Apoptotic and necrotic cells were counted under a fluorescence microscope. *E,* The cells described in (*D*) were further transfected with a pro-IL-1β-expressing plasmid. After 21 h, the cells were treated with MDP (1000 ng/ml) for 3 h, and IL-1β in the culture supernatant was measured by ELISA. *Error bars* in *B, D* and *E* indicate S.D.

FIGURE 7. Caspase-1, but not its catalytic activity, is required for the necrotic cell death of monocytes infected with bacteria. *A* and *G*, Optical phase contrast images of NOMO-1 cells either uninfected (left panels), or infected with *S. aureus* (*A*, right panel) or *P. aeruginosa* (*G*, right panel) at an moi of 20 for 4 h. Scale bar, 20 μm. *B* and *H*, NOMO-1 cells were transfected with control, ASC-, NLRP3-, or NLRC4-targeting siRNA. After 72 h, the cells were infected with *S. aureus* (*B*, moi 20 or 50) for 2 h, or with *P. aeruginosa* (*H*, moi 50) for 4 h. The knockdown efficiency was examined by RT-PCR (*B*, right panels). *C,* NOMO-1 cells were pre-treated with 20 μM of the indicated inhibitors for 1 h. Cells were then infected with *S. aureus* for 2 h. *D* and *J*, NOMO-1 cells were pre-treated with the indicated concentrations of Ac-YVAD-CMK for 1 h. The cells were then infected with *S. aureus* (moi 20) for 2 h (*D*), or with *P. aeruginosa* (moi 50) for 4 h (*J*). *E* and *I*, NOMO1-shCont and NOMO1-shCasp1 cells were infected with *S. aureus* (moi 50) for 2 h (*E*), or *P. aeruginosa* (moi 50) for 4 h (*I*). *F,* NOMO-1 cells were transfected with control (Cont) or caspase-1-targeting siRNA (C1) 1–3 times at 4-day intervals. At 4, 8, or 12 days after the first transfection, the cells were infected with *S. aureus* (moi 20) for 2 h. Caspase-1 and GAPDH levels at the end of a 4-, 8- or 12-day culture before infection were examined by Western blotting. *B-F* and *H-J*, Cytotoxicity was assessed by LDH release assays. The amount of IL-1β in culture supernatants was examined by ELISA. % of control = (value of cells treated with Ac-YVAD-CMK or caspase-1-targeting siRNA /value of cells treated with the solvent control or control siRNA) x 100. *Error bars* in *B-F* and *H-J* indicate S.D.

Fig. 1

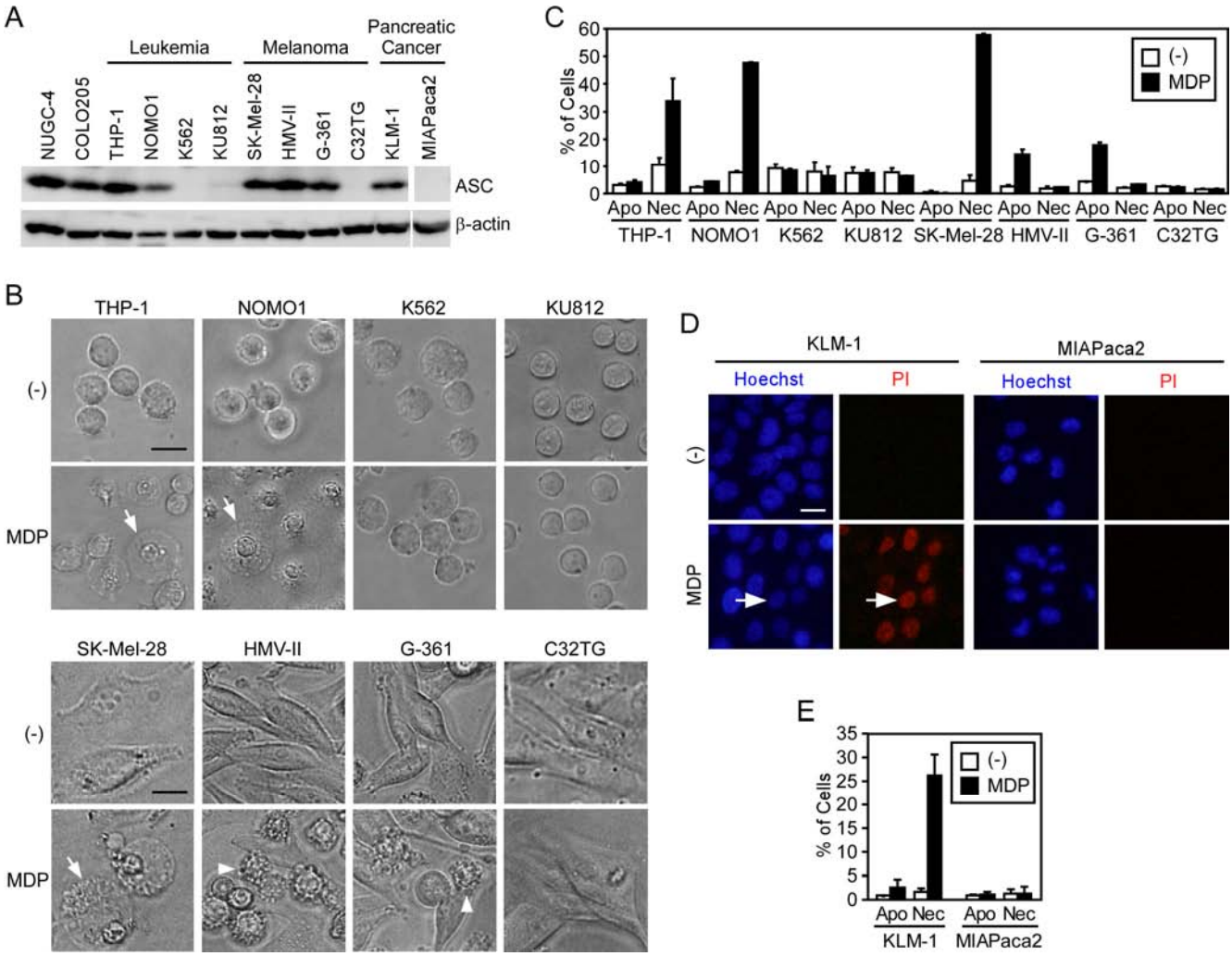
A
Leukemia
Melanoma
Pancreatic Cancer
NUGC-4
COLO205
THP-1
NOMO1
K562
KU812
SK-Mel-28
HMV-II
G-361
C32TG
KLM-1
MIAPaca2
ASC
β-actin
C
% of Cells
(-)
MDP
Apo Nec
THP-1
NOMO1
K562
KU812
SK-Mel-28
HMV-II
G-361
C32TG
B
(-)
MDP
D
KLM-1
MIAPaca2
Hoechst
PI
E
KLM-1
MIAPaca2

Fig. 2

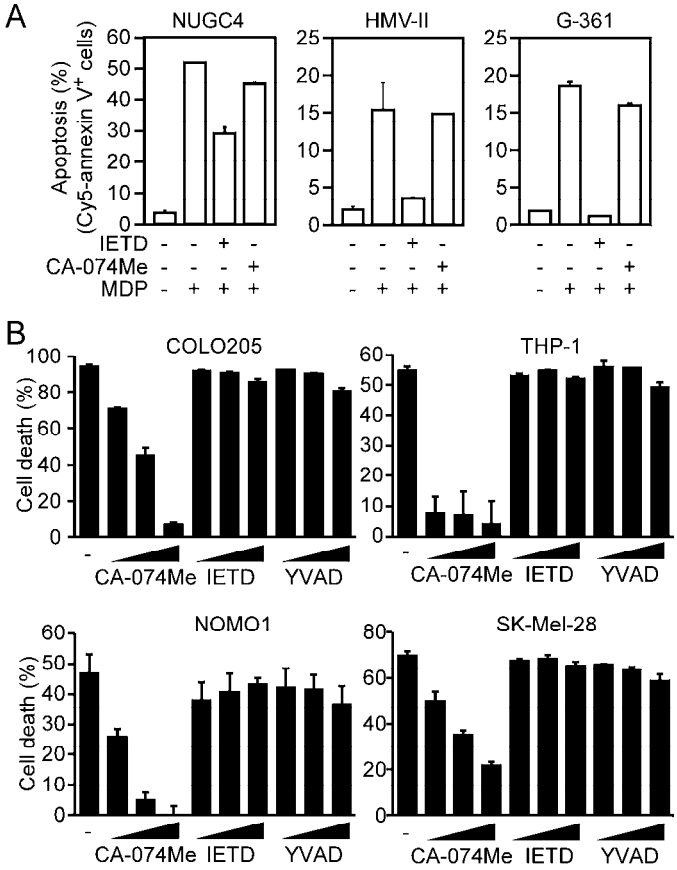
A
NUGC4
HMV-II
G-361
Apoptosis (%)
(Cy5-annexin V+ cells)
IETD
CA-074Me
MDP
B
COLO205
THP-1
NOMO1
SK-Mel-28
Cell death (%)
CA-074Me
IETD
YVAD

Fig. 3

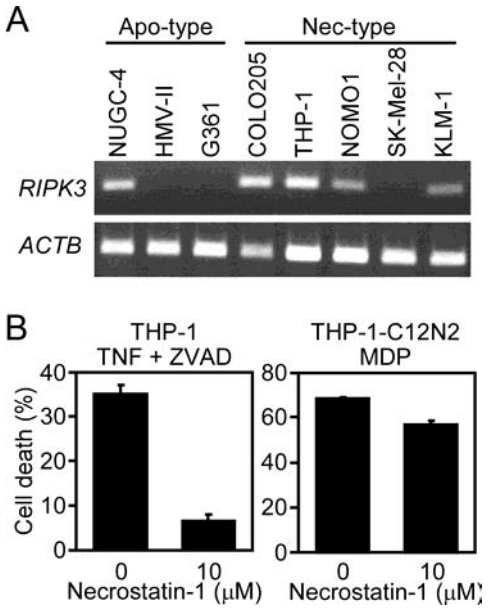
A
Apo-type
Nec-type
NUGC-4
HMV-II
G361
COLO205
THP-1
NOMO1
SK-Mel-28
KLM-1
RIPK3
ACTB
B
THP-1
TNF + ZVAD
THP-1-C12N2
MDP
Cell death (%)
Necrostatin-1 (μM)

Fig. 4

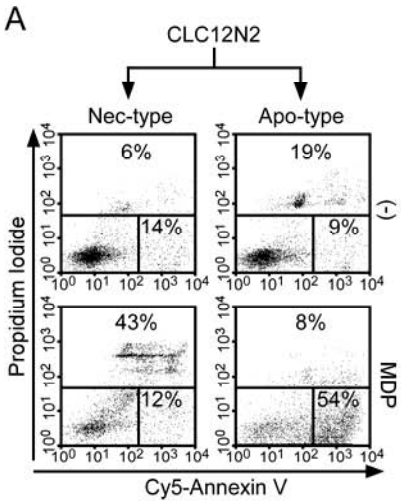

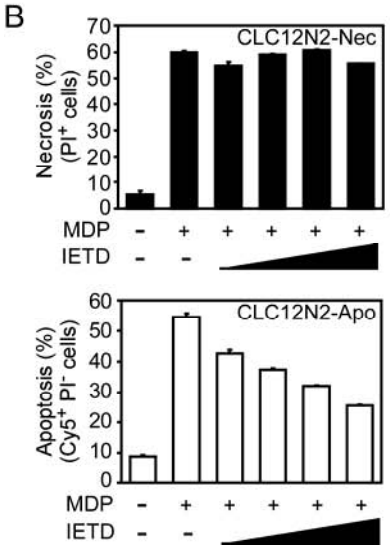

C

Top 10 genes expressing more in CLC12N2-Nec than CLC12N2-Apo Cells

Gene Name	CLC12N2-Nec vs CLC12N2-Apo (Fold)	COLO205 (Nec) vs NUGC-4 (Apo) (Fold)
FZD10	58.61	57.70
SPINK1	45.04	22.73
CASP1	26.53	67.23
CALB1	18.95	19.10
DPEP1	15.43	3.14
CARD16	13.76	29.85
CARD17	9.04	17.30
CTSS	6.40	24.52
BTNL3	6.29	24.52
CD244	5.80	12.23

Top 10 genes expressing more in CLC12N2-Apo than CLC12N2-Nec Cells

Gene Name	CLC12N2-Apo vs CLC12N2-Nec (Fold)	NUGC-4 (Apo) vs COLO205 (Nec) (Fold)
SERPINE2	6.02	2.13
GPSM1	5.62	13.09
HOMER3	4.41	5.47
MIA	4.36	6.32
CCNG2	4.09	4.27
NCS1	3.85	16.87
ARHGEF26	3.72	6.35
SMARCA1	3.69	3.79
AQP5	3.61	7.43
SRPX2	3.32	9.03

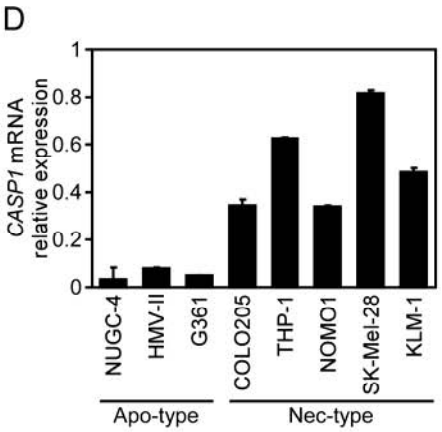

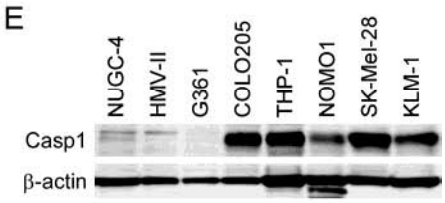

Fig. 5

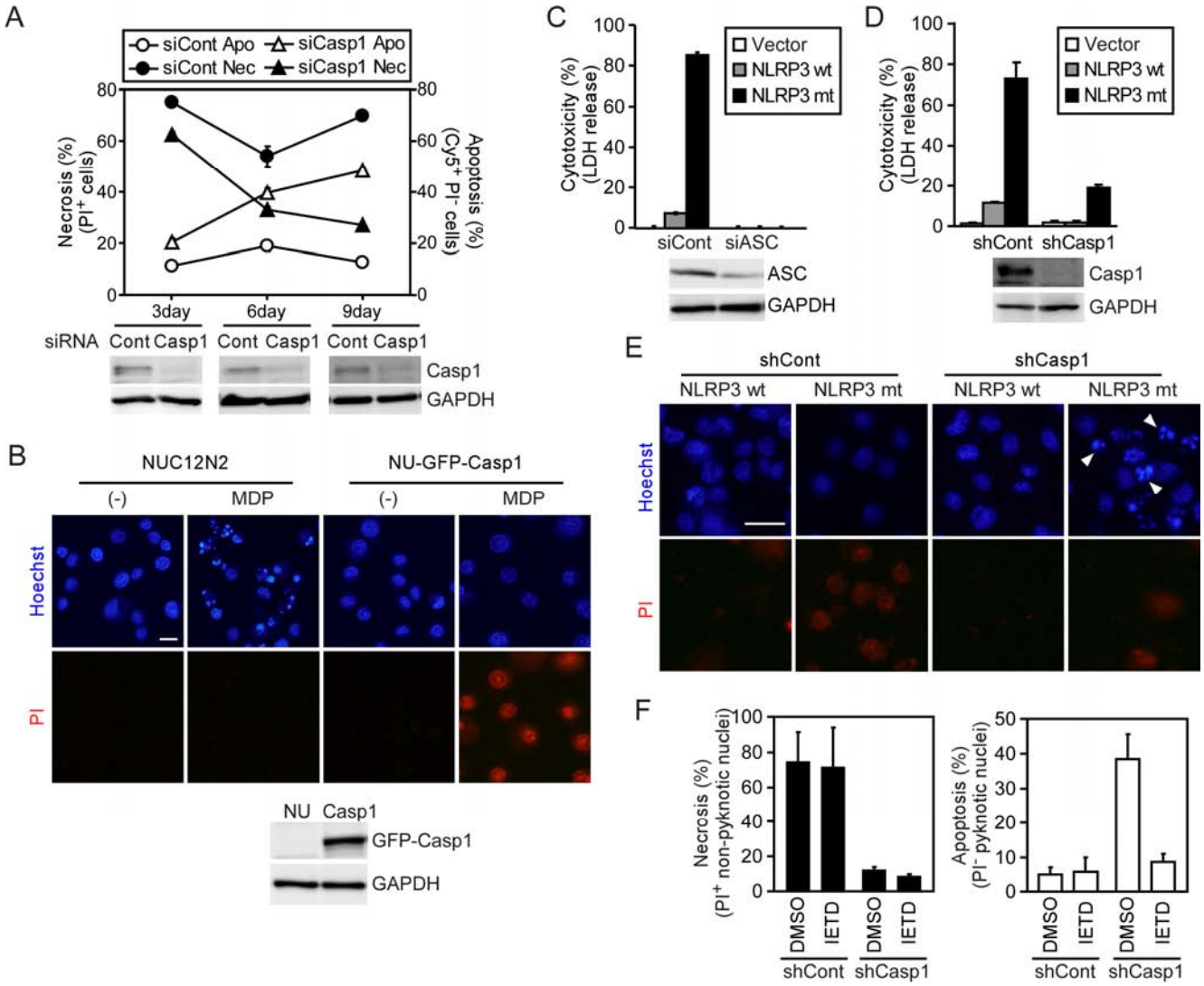
A
siCont Apo
siCasp1 Apo
siCont Nec
siCasp1 Nec
Necrosis (%) (PI+ cells)
Apoptosis (%) (Cy5+ PI- cells)
3day
6day
9day
siRNA Cont Casp1 Cont Casp1 Cont Casp1
Casp1
GAPDH
B
NUC12N2
NU-GFP-Casp1
(-)
MDP
Hoechst
PI
NU Casp1
GFP-Casp1
GAPDH
C
Vector
NLRP3 wt
NLRP3 mt
Cytotoxicity (%) (LDH release)
siCont siASC
ASC
GAPDH
D
shCont shCasp1
Casp1
GAPDH
E
shCont
shCasp1
NLRP3 wt
NLRP3 mt
F
Necrosis (%) (PI+ non-pyknotic nuclei)
Apoptosis (%) (PI- pyknotic nuclei)
DMSO
IETD

Fig. 6

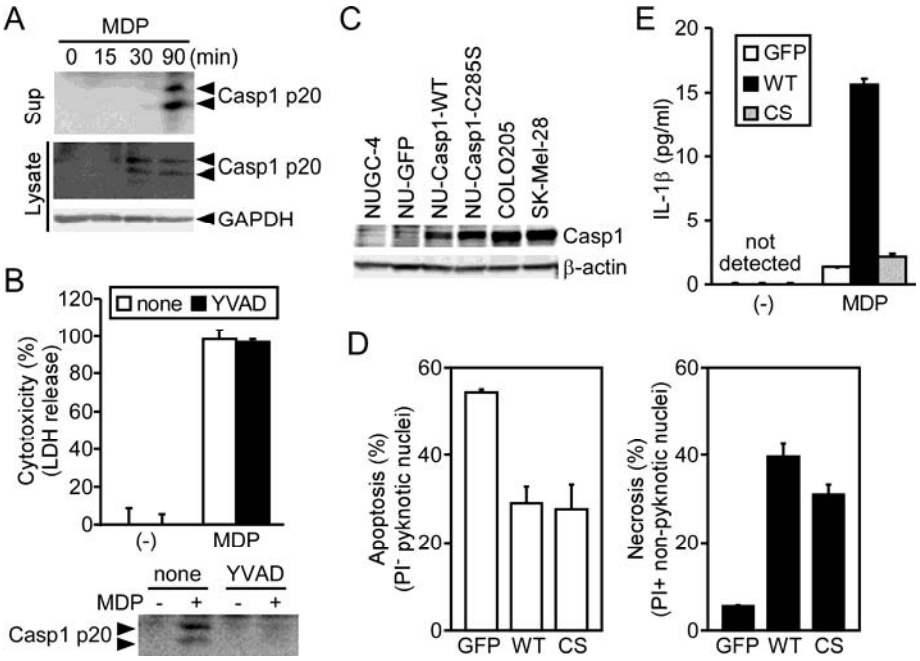
A
MDP
0 15 30 90 (min)
Sup
Casp1 p20
Lysate
Casp1 p20
GAPDH
B
none YVAD
Cytotoxicity (%) (LDH release)
120
100
80
60
40
20
0
(-)
MDP
none
YVAD
MDP - + - +
Casp1 p20
C
NUGC-4
NU-GFP
NU-Casp1-WT
NU-Casp1-C285S
COLO205
SK-Mel-28
Casp1
β-actin
D
Apoptosis (%) (PI- pyknotic nuclei)
60
40
20
0
GFP WT CS
Necrosis (%) (PI+ non-pyknotic nuclei)
60
40
20
0
GFP WT CS
E
IL-1β (pg/ml)
20
15
10
5
0
GFP
WT
CS
not detected
(-)
MDP

Fig. 7

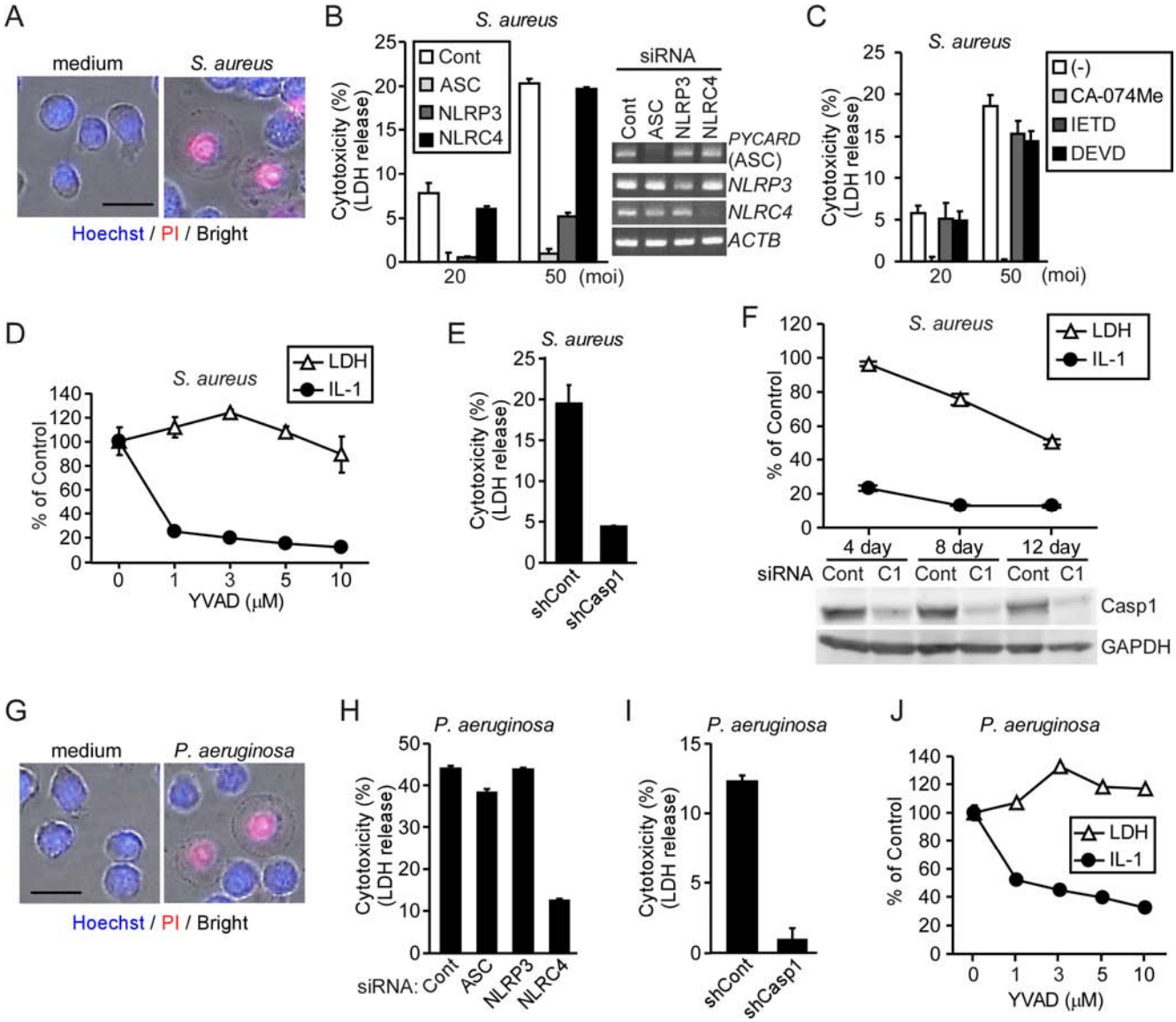
A
medium
S. aureus
Hoechst / PI / Bright
B
S. aureus
Cytotoxicity (%) (LDH release)
Cont
ASC
NLRP3
NLRC4
siRNA
Cont
ASC
NLRP3
NLRC4
PYCARD (ASC)
NLRP3
NLRC4
ACTB
20
50 (moi)
C
S. aureus
Cytotoxicity (%) (LDH release)
(-)
CA-074Me
IETD
DEVD
20
50 (moi)
D
S. aureus
LDH
IL-1
% of Control
YVAD (μM)
E
S. aureus
Cytotoxicity (%) (LDH release)
shCont
shCasp1
F
S. aureus
LDH
IL-1
% of Control
4 day
8 day
12 day
siRNA Cont C1 Cont C1 Cont C1
Casp1
GAPDH
G
medium
P. aeruginosa
Hoechst / PI / Bright
H
P. aeruginosa
Cytotoxicity (%) (LDH release)
siRNA: Cont
ASC
NLRP3
NLRC4
I
P. aeruginosa
Cytotoxicity (%) (LDH release)
shCont
shCasp1
J
P. aeruginosa
% of Control
LDH
IL-1
YVAD (μM)

Supplementary Videos

Video S1. CLC12N2-Nec cells were treated with MDP (100 ng/ml). Starting 3 h after the MDP addition, images were captured every 7.5 s for 25 min and are displayed at 500 frames/ min.

Video S2. CLC12N2-Apo cells were treated with MDP (100 ng/ml). Starting 3 h after the MDP addition, images were captured every minute for 3 h and are displayed at 500 frames/min.

Supplementary Figures

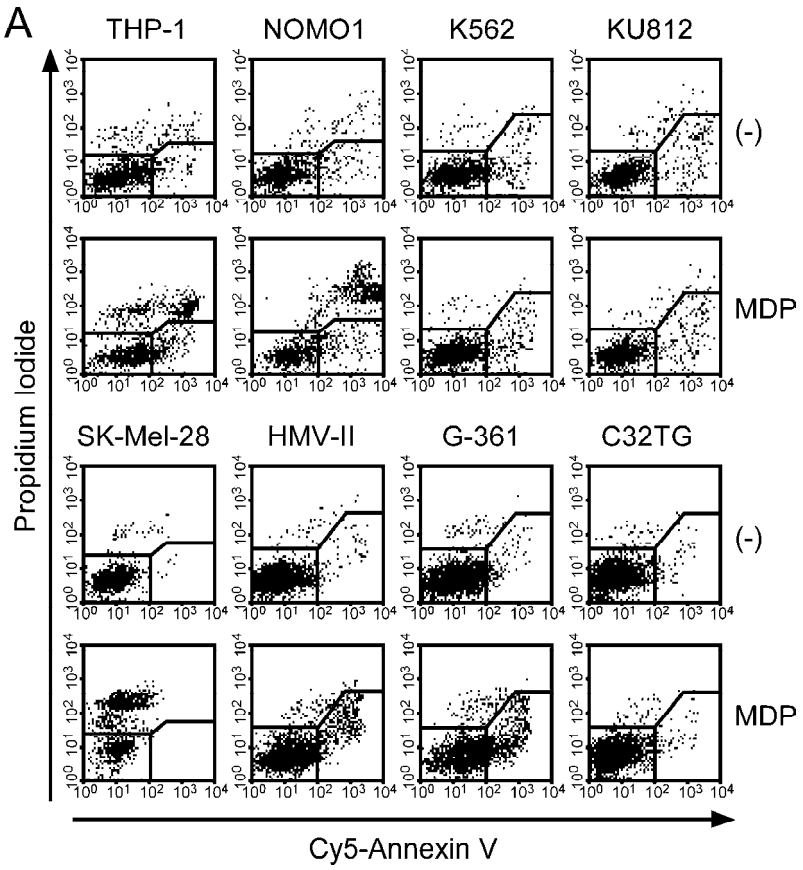

FIGURE S1. **ASC activation induces apoptosis or necrosis.** *A*, Two-dimensional (propidium iodide and Cy5-annexin V) staining profiles of the cells described in Fig. 1*C*. *B*, Time course of the staining profiles of apoptosis-type cells after MDP addition. *A* and *B*, MDP-treated THP-1, NOMO-1, and SK-Mel-28 cells exhibited increased PI staining preceding or occurring simultaneously with increased Cy5-Annexin V staining. Therefore, the PI(+) Cy5-Annexin V(+) cells were considered necrotic cells. On the other hand, MDP-treated HMV-II and G-361 cells exhibited an increase in Cy5-Annexin V staining that preceded PI staining. Thus, the PI(+) Cy5-Annexin V(+) cells were considered apoptotic cells. The morphology of the dying cells (Fig. 1*B*) and the fact that pretreatment with Z-IETD-FMK inhibited the development of PI(+) Cy5-Annexin V(+) cells from the latter cell lines but not from the former cell lines (Fig. 2) support this evaluation.

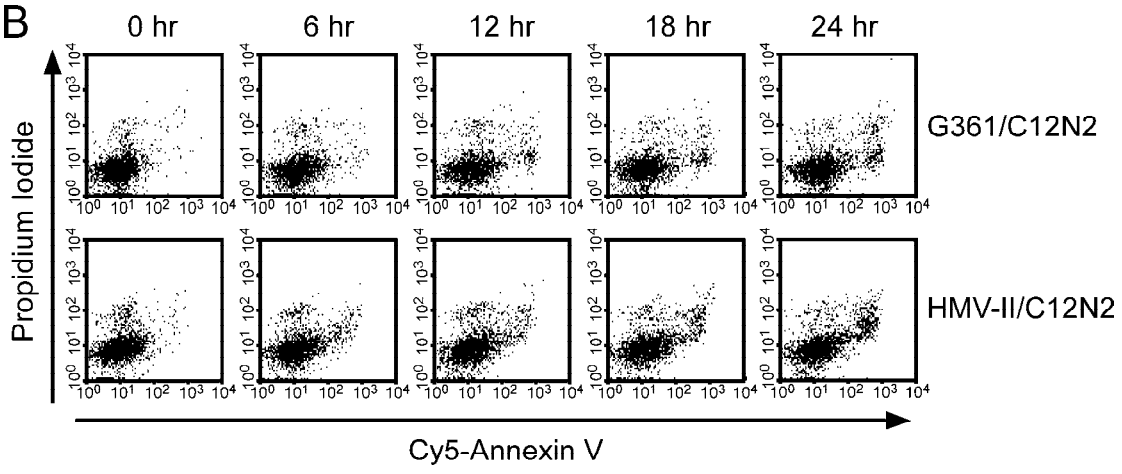

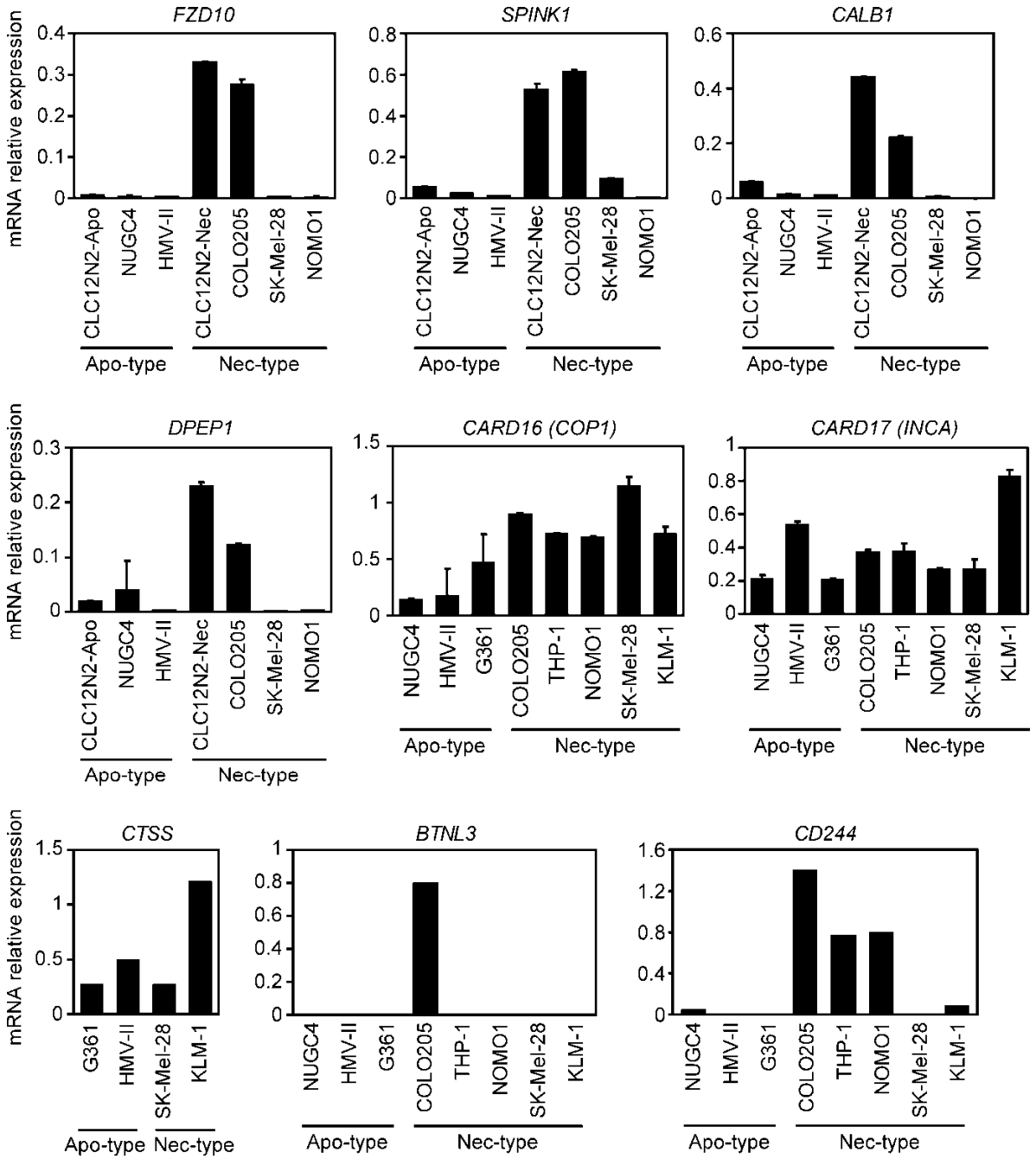

FIGURE S2. **The mRNA expression levels in apoptosis-type and necrosis-type cell lines of the genes listed in the upper panel of Fig. 1*C*.** The mRNA levels of the indicated genes were analyzed by real-time PCR. Relative mRNA expression levels normalized to that of *ACTB* (β-Actin) are shown. The primer sequences are shown in supplementary Table S1. *FZD10*, frizzled homolog 10; *SPINK1*, serine peptidase inhibitor, Kazal type 1; *CALB1*, calbindin 1; *DPEP1*, dipeptidase 1; *CARD16*, caspase recruitment domain family, member 16 (also known as COP1); *CARD17*, caspase recruitment domain family, member 17 (also known as INCA); *CTSS*, cathepsin S; BTNL3, butyrophilin-like 3; *CD244*, CD244 molecule, natural killer cell receptor 2B4.

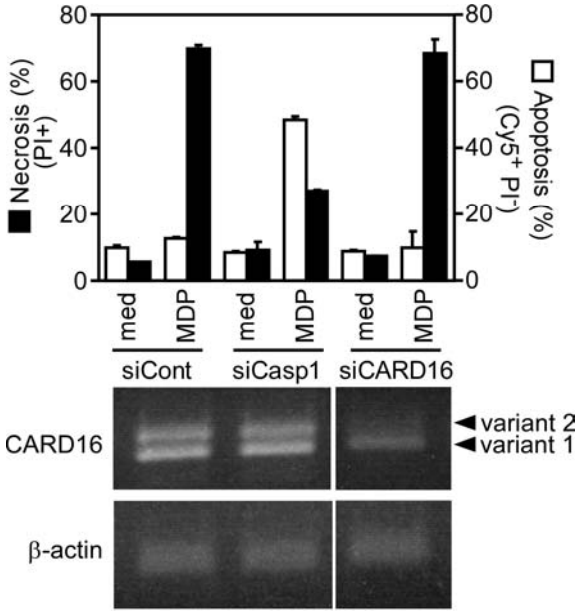

FIGURE S3. **CARD16 knockdown in CLC12N2-Nec cells does not convert the cell death mode.** CLC12N2-Nec cells were transfected with control, caspase-1-targeting, or *CARD16*-targeting siRNA (Invitrogen, HSS174333) on days 0, 3, and 6. On day 9, the cells were treated with MDP (100 ng/ml) for 12 h, and the proportions of apoptotic and necrotic cells were determined by flow cytometry as described in Fig. 1*B*. The expression levels of *CARD16* and *ACTB* (β-actin) on day 8 were examined by RT-PCR (lower panels). The following primers were used for PCR: *CARD16*, 5'-GCCATGGCCGACAAGGT-3' and 5'-ACCTAGGAAGGAAGTACTATTTGAG-3'; β-actin, 5'-TCCCTGGAGAAGAGCTACGA-3' and 5'-AAAGCCATGCCAATCTCATC-3'.

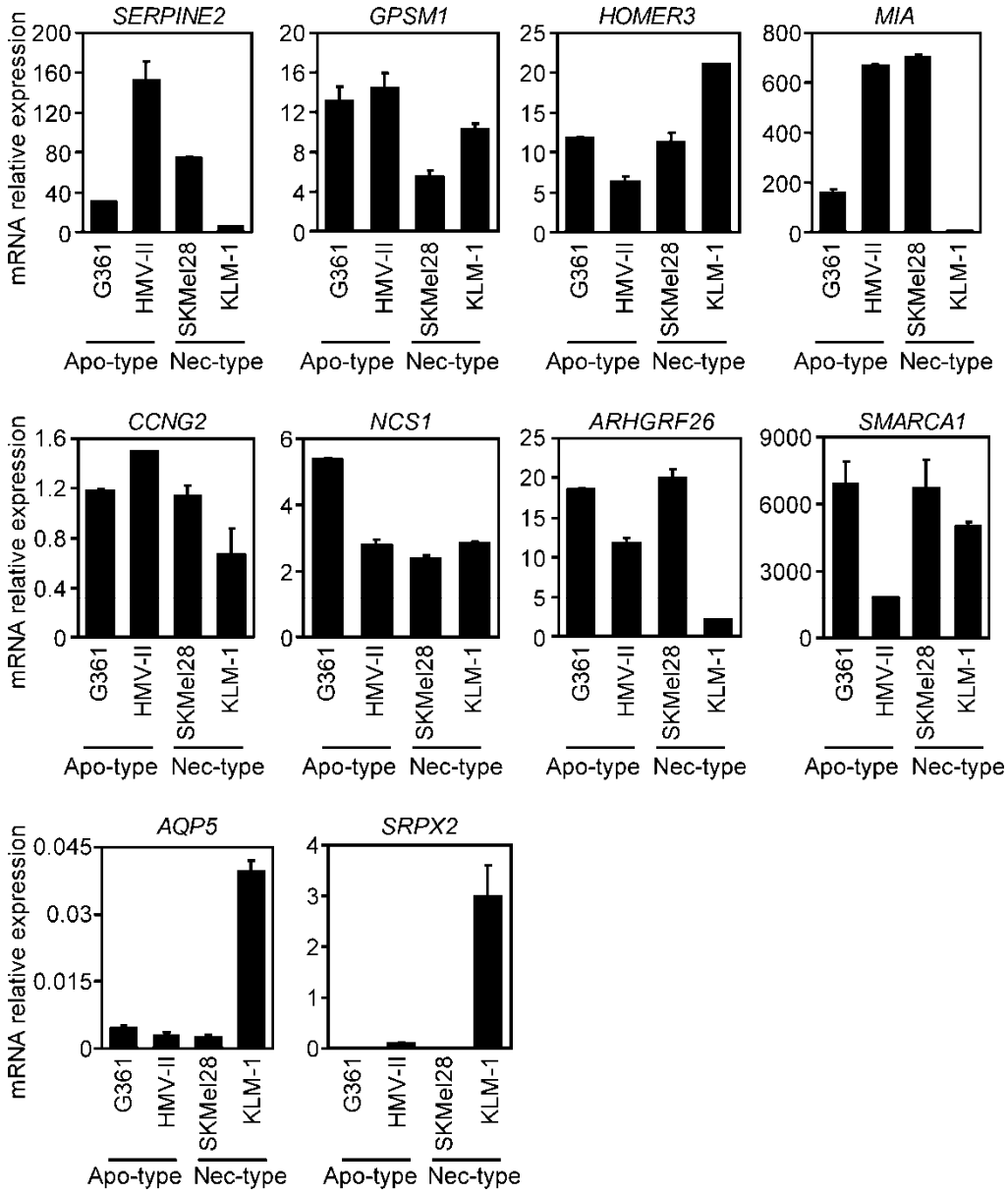

FIGURE S4. **The mRNA expression levels in apoptosis-type and necrosis-type cell lines of the genes listed in the lower panel of Fig. 1*C*.** The mRNA levels of the indicated genes were analyzed by real-time PCR. Relative mRNA expression levels normalized to that of *ACTB* (β-Actin) are shown. The primer sequences are shown in supplementary Table S1. *SERPINE2*, serpin peptidase inhibitor, clade E, member 2; *GPSM1*, G-protein signaling modulator 1; *HOMER3*, homer homolog 3; *MIA*, melanoma inhibitory activity; *CCNG2*, cyclin G2; *NCS1*, neuronal calcium sensor 1; *ARHGEF26*, Rho guanine nucleotide exchange factor 26; *SMARCA1*, SWI/SNF related, matrix associated, actin dependent regulator of chromatin, subfamily a, member 1; *AQP5*, aquaporin 5; *SRPX2*, sushi-repeat-containing protein, X-linked 2.

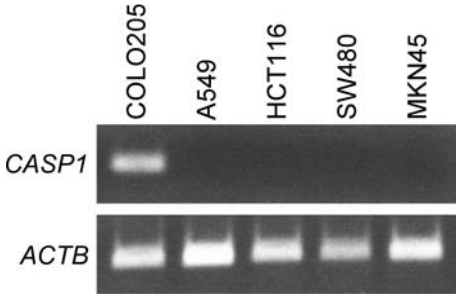

FIGURE S5. **Apoptosis-type cells do not express caspase-1.** RT-PCR was used to examine caspase-1 and β-actin mRNA expression in four human cancer cell lines (A549, HCT116, SW480, MKN45) that exhibit apoptosis in response to ASC activation by NLRC4-mimicry.

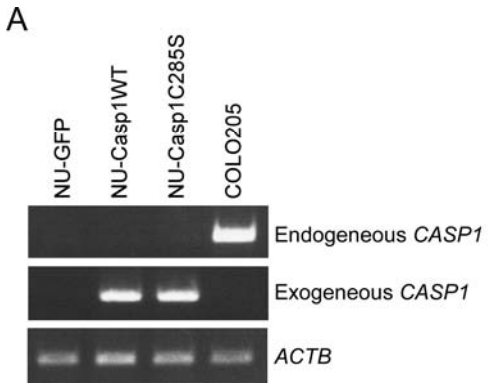

FIGURE S6. **The catalytic activity of caspase-1 is not required for ASC-mediated necrosis.** *A*, Total RNA was isolated from the indicated cell lines, and the mRNA levels of endogenous and exogenous caspse-1 and β-actin were detected by RT-PCR. *B*, NU-GFP, NU-Casp1WT, and NU-Casp1C285S cells were cultured with MDP (1000 ng/ml) for 6 h. Cytotoxicity was assessed by LDH release assay.

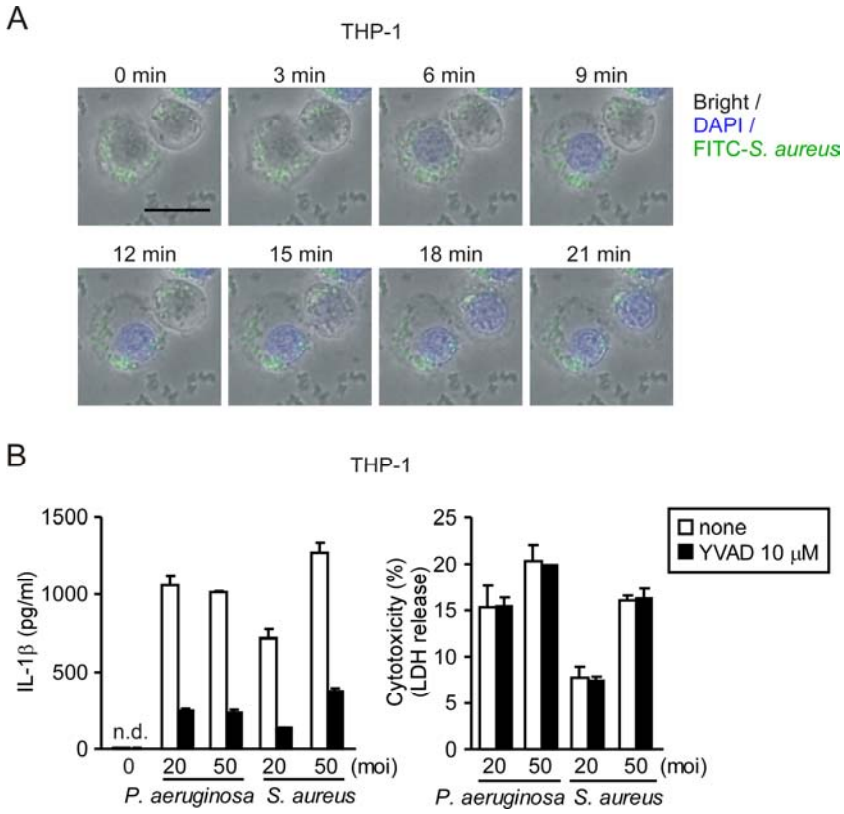

FIGURE S7. **Ac-YVAD-CMK inhibits the IL-1β release but not the necrosis induced by bacterial infection in THP-1 cells.** *A*, THP-1 cells were treated with PMA (10 ng/ml) for 12 h to allow cells to adhere to the culture plate, and the cells were then infected with FITC-labeled *S. aureus* (moi 50) in the presence of 4',6-diamidino-2-phenylindole (DAPI). Time-lapse images were recorded every 3 min beginning 3 h after infection. Scale bar, 20 μm. Nuclear staining with DAPI and the swelling of *S. aureus*-infected cells indicates that *S. aureus* induced necrosis in THP-1 cells. *B*, THP-1 cells were pretreated with Ac-YVAD-CMK (10 μM) for 1 h, and then infected with *S. aureus* for 2 h or with *P. aeruginosa* for 4 h. The culture supernatants were examined for LDH and IL-1β release.

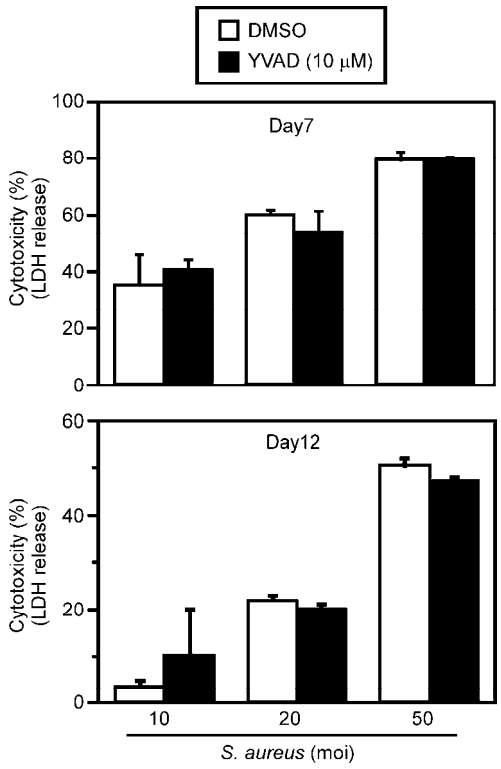

FIGURE S8. **Long-term inhibition of caspase-1 activity does not supress *S. aureus*-induced necrosis of NOMO-1 cells.** NOMO-1 cells were treated with Ac-YVAD-CMK for 7 or 12 days. Cells were then infected with *S. aureus* at the indicated moi in the presence of Ac-YVAD-CMK for 4 h. Cytotoxicity was assessed by LDH release assays.

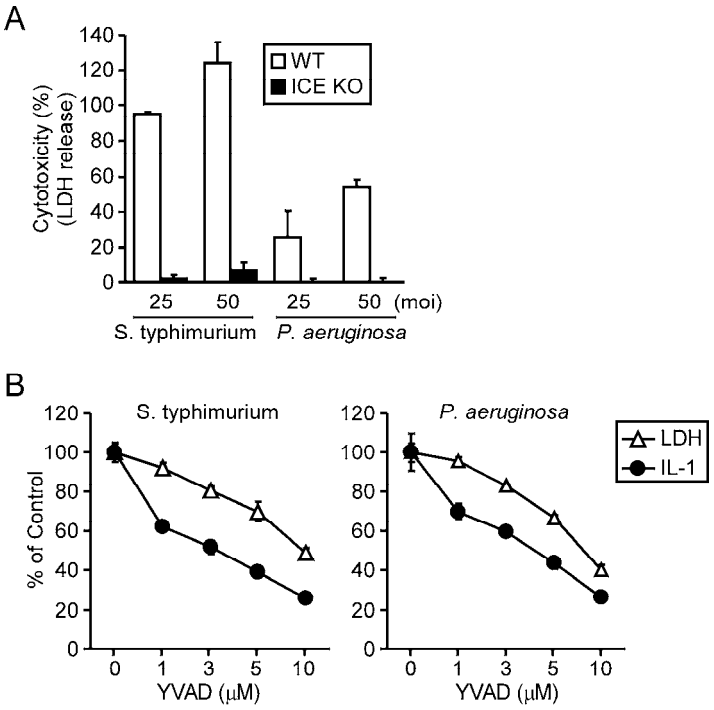

FIGURE S9. **Caspase-1 catalytic activity seems to be required for pyroptosis of mouse macrophages.** *A*, Thioglycollate-induced peritoneal macrophages were prepared from wild-type (WT, Caspase-$1^{+/+}$) or ICE KO (Caspase-$1^{-/-}$) mice. The macrophages were primed with LPS (100 ng/ml) for 12 h, and then infected with *Salmonella* (*S.*) *typhimurium* (ATCC 14028s) or *P. aeruginosa* for 2 h. *B*, Thioglycollate-induced peritoneal macrophages from wild-type mice were primed with LPS (100 ng/ml) for 4 h. The LPS-primed macrophages were pre-treated with the indicated concentrations of Ac-YVAD-CMK for 1 h, and then infected with *S. typhimurium* or *P. aeruginosa* for 1 h. LDH release and IL-1β production were analyzed as described in Fig. 7.

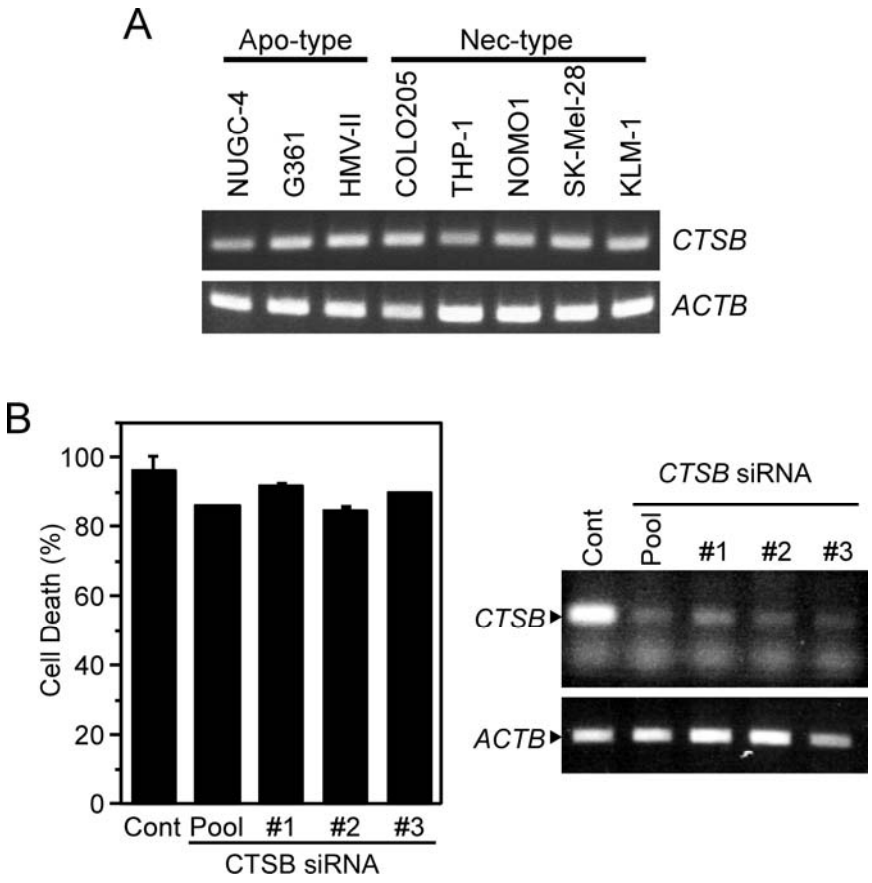

FIGURE S10. Cathepsin B may not be the target of CA-074Me in the inhibition of ASC-mediated necrosis. *A*, Total RNA was extracted from the indicated cell lines, and the expression of cathepsin B mRNA (*CTSB*) was examined by RT-PCR analysis. *B*, NOMO1-C12N2 cells were transfected with 20 nM of a control siRNA, a pool of four *CTSB* siRNAs (Dharmacon, L-004266-00), or three individual *CTSB* siRNAs (invitrogen, HSS102475-7). Forty eight hours later, cells were treated with MDP (300 ng/ml) for 6 h. Cell death was assessed by WST-1 assays (left panel). Knockdown of cathepsin B mRNA was confirmed by RT-PCR analyses (right panels).

Supplementary table

Table S1. The primer sequences[1)] used in Fig. S2 and S4.

Gene	Sense	Antisense
FZD10	CGGTGAAGACCATCCTGATCC	CAGCTTGTCCGTGTTCTCG
CD244	AAGCCACACCCTGAATCTCAC	CCAAAAACGGCCAAAATCTGAA
SPINK1	AGTCTATCTGGTAACACTGGAGC	ACACGCATTCATTGGGATAAGT
CALB1	AGGGAATCAAAATGTGTGGGAAA	TCCTTCAGTAAAGCATCCAGTTC
DPEP1	AGAGCCCCGGTCATCTTCA	CCTTGTTGGTGCAGGAAATGTA
CARD16	TGCAGAGGTGCCATGTTCAG	TTTATGCAAGGGGAGCAGCAGAAG
CARD17	AATGGCTTACTGGGTGAATTATTGG	TGTGATGCAAATTTGGCATGCTGGA
CTSS	ATGAAACGGCTGGTTTGTGTG	TGCTCCAGGTTGTGAAGCATC
BTNL3	GGGGCGTGTCTCTCTAAGG	CGTCAACATATCCCACGATGGA
SERPINE2	ACGCCGTGTTTGTTAAGAATGC	CGTTGACGAGGACCAGTCT
GPSM1	GGAGCCGGGCCTATCTCTAAA	CTCTTGCTGCCAGTAAGCATC
HOMER3	GGCGAGGAAAAACTGTTCCG	ACAACATCTTCTTTAGCCGCTC
MIA	GTCAGGGGTGGTCCTATGC	GGTCAGGAATCGGCAGTCG
CCNG2	TGCCTAGCCGAGTATTCTTCT	TGTTTGTGCCACTTTGAAGTTG
NCS1	TTCAAGCTCTACGACTTGGACA	GCTCCACGGTATTCCCCAC
ARHGEF26	CCGTGGTTTTGAGTACAAACAGC	CGCACCTTGAGGAGTCTCTTG
SMARCA1	GATGCGACCGCCACTATCG	AGATTTAGGCGCTTTAGCAGC
AQP5	CTGTCCATTGGCCTGTCTGTC	GGCTCATACGTGCCTTTGATG
SRPX2	GATGAGATGCCACGCACTACC	TCTTCCATGCAGATTCGGCTG

1) These primer sequences, with the exception of those for *CARD16* and *CARD17,* were obtained from PrimerBank (http://pga.mgh.harvard.edu/primerbank/).